Arclogites in the subarc lower crust: effects of crystallization, partial melting, and retained melt on the foundering ability of residual roots

Emilie E. Bowman[1*], Mihai N. Ducea[1,2], and Antoine Triantafyllou[1,3]

[1]Department of Geosciences, University of Arizona, Tucson, AZ 85721, USA

[2]Faculty of Geology and Geophysics, University of Bucharest, Bucharest, 010040 Romania

[3]Geology Laboratory of Lyon – Earth, Planets and Environment (LGL-TPE), Université de Lyon, Université Lyon 1, ENS de Lyon, CNRS, UMR 5276, F-69622 Villeurbanne, France.

[*]corresponding author. E-mail: eebowman@email.arizona.edu

ABSTRACT

Thick-crusted (>45 km) Cordilleran arcs exhibit cyclic processes including periods of magmatic quiescence interspersed with pulses of high-flux magmatism. Most models assume that during high-flux events, fractional crystallization and partial melting within the deep crustal hot zone generate a dense (>3.4 g/cm^3) arclogitic subarc root that can readily founder into the mantle. Yet these models do not consider that (1) the retention of low-density melt within the subarc root and (2) the protolith lithology of the restitic portion of the subarc root may greatly impact the density evolution of the root and its susceptibility to foundering. In this paper, we first address the effect of retained melt on the foundering ability of the subarc root by calculating the density and time for foundering of melt-bearing arclogitic residue at 1.5, 2, and 2.5 GPa. We find that melt volumes >10-18% are required to stabilize the root within the lower crust; melt volumes below this threshold lower the viscosity of the residue so much so as to decrease the time for foundering by an order of magnitude. We then constrain through phase equilibria modeling the effect of partial melting of different lower crustal protoliths on the density of the restitic subarc root. To do this, we model the density and mineralogical evolution of restites in equilibrium with their derivative melts during open-system, isobaric partial melting of typical crustal assemblages from 600-1100^{o}C at 1.5 (~50 km) and 2 GPa (~65 km). In our models, typical end-member assemblages in a lower crustal hot zone include basalt, metapelite, and metagraywacke. We find that melt-depleted restites derived from basaltic compositions are amphibole-bearing arclogites with densities conducive to foundering, which at 2 GPa can occur even in the presence of the coexisting hydrous felsic residual melt. Foundering of the amphibole ± melt-bearing root may refertilize the mantle wedge and induce melting of the surrounding asthenosphere as well as the arclogitic mass. However, if temperatures in a 50-km deep subarc hot zone are not sufficient to drive melt depletion of basaltic restites, these dense (3.1-3.3 g/cm^3) residues are gravitationally

stable, increasing the density of the lower crust and lowering the elevation of the arc. In comparison, partial melting of metasedimentary country rock produces alkali feldspar-rich residues that never achieve densities conducive to foundering. Thus, if high-flux events are driven by the influx of melt-fertile lithosphere beneath the arc as envisioned by the Cordilleran cycle model, then partial melting of the metasedimentary portion will generate low-density residues that remain in the lower crust and contribute to the thickness, geochemistry, and seismic structure of the bulk arc.

Keywords: arclogite; Cordilleran arc; deep crustal hot zone; foundering; partial melting

INTRODUCTION

Cordilleran orogenic systems form where oceanic subduction beneath continental crust generates widespread deformation, metamorphism, and magmatism. These systems, best exemplified by the modern Andes and the exhumed North American Cordillera, are distinct from other subduction zones in that a compressional stress regime prevails, driving retroarc shortening and generating overly thickened (up to 75 km) continental crust (Allmendinger *et al*., 1997). As such, paralleling the subduction zone are high-elevation (>4 km) magmatic arcs and back-arc orogenic plateaus that heavily influence ocean circulation, biodiversity, species evolution, and global climate (Sepulchre *et al*., 2009; Hoorn *et al*., 2010; Luebert & Muller, 2015). The magmatic arc further generates large volumes of intermediate calc-alkaline magmas that not only produce the extensive linear batholiths and stratovolcanoes exposed within these systems (Ducea *et al*., 2015) but also play a critical role in building the continental crust as a whole (Jagoutz & Kelemen,

2015). A portion of these batholiths are enriched in precious metals and host well-endowed ore deposits (Richards, 2011).

Based on previous studies of the North (e.g. Ducea & Saleeby, 1998; Manley *et al*., 2000; Farmer *et al*., 2002; Jones *et al*., 2004; Gehrels *et al*., 2009) and South American Cordilleras (DeCelles *et al*., 2015a and references therein), it is clear that Cordilleran arcs are long-lived features characterized by cycles of linked intra-arc processes including periods of voluminous magmatism separated by magmatic lulls as well as convective removal of dense subarc roots, topographic uplift, and crustal deformation (Ducea *et al*., 2015). Several models have been proposed to describe how Cordilleran subduction systems form and evolve under such periodicity, one of the most holistic being the Cordilleran cycle model of DeCelles *et al*. (2009) (Fig. 1a). This model asserts that shortening in the retroarc thrust belt must be accompanied by underthrusting of foreland lithosphere into the subarc region. Emplacement of foreland lithosphere to greater depths not only promotes crustal thickening but also transports melt-fertile materials, such as felsic to intermediate continental crust (Clemens & Vielzeuf, 1987) and refertilized lithospheric mantle (Chapman *et al*., 2021), into the deep crustal hot zone of the frontal arc (Fig. 1b). Because such melt-fertile lithologies are hydrous, fusible element-rich assemblages, these rocks have lower solidus temperatures and higher melt productivities compared to more refractory compositions (Clemens & Vielzeuf, 1987; Langmuir *et al*., 1992). The delivery of foreland lithosphere beneath the arc therefore leads to higher extents of melting (Ducea & Barton, 2007). As a result, superimposed onto background levels of magmatism (<20 km^3 magmatic volume/km arc-length/Myr) sourced from the mantle wedge are 1-25 million year-long pulses of high-flux magmatism (~70-90 km^3/km/Myr) derived in part from the continental lithosphere (Ratschbacher *et al*., 2019; Chapman *et al*., 2021).

The majority of Cordilleran batholiths are generated during high-flux magmatic events. Magma flare-ups manifest as peaks on probability density plots of batholith-derived zircon U-Pb ages (Kirsch *et al*., 2016 and references therein), which are separated by troughs representing magmatic lulls. Consistent with retroarc underthrusting as a driver of high-flux magmatism, batholiths emplaced during flare-ups typically display $^{143}Nd/^{144}Nd$ and $^{176}Hf/^{177}Hf$ decreases as well as $^{87}Sr/^{86}Sr$ increases indicating incorporation of old, evolved lithosphere into the magmatic budget (Haschke *et al*., 2002; Ducea & Barton, 2007; DeCelles *et al*., 2009). Landward arc migration may provide another mechanism for delivering fertile lithosphere into the hot zone and inciting magma flare-ups (Chapman & Ducea, 2019). In this case, magmatism during high-flux events need not exhibit isotopic excursions if juvenile rather than evolved crustal material is forced into the hot zone.

Under the thickest volcanic arcs, such as the central Andes today (McGlashan *et al*., 2008), partial melting of underthrusted material during high-flux events has been proposed to generate a restitic garnet pyroxenitic, or "arclogitic" (Lee & Anderson, 2015), lower crustal and mantle lithospheric root that is denser (>3.4 g/cm^3; Ducea, 2002; Lee *et al*., 2006) than the underlying mantle (3.25-3.35 g/cm^3; Poudjom Djomani *et al*., 2001; Kelly *et al*., 2003). This root takes up space in the mantle wedge, restricts further retroarc underthrusting, and creates a negative buoyancy force that drives surface subsidence (Fig. 1a; Pysklywec & Cruden, 2004; Göğüş & Pysklywec, 2008; DeCelles *et al*., 2009). Once the dense root exceeds a critical thickness (Behn *et al*., 2007), it begins to founder into the underlying mantle (Kay & Kay, 1993; Ducea & Saleeby, 1998). Detachment and sinking of the residual root and concomitant asthenospheric upwelling induce ~1 km of rapid (0.15-1 mm/yr) uplift of the overlying arc and hinterland region (Jones *et al*., 2004; Garzione *et al*., 2006; Ghosh *et al*., 2006; Le Pourhiet *et al*., 2006; Garzione *et al*., 2008; Göğüş & Pysklywec, 2008; Krystopowicz & Currie, 2013; Lee,

2014; Currie *et al*., 2015). Uplift drives hinterland extension, local basaltic volcanism, and foreward propagation of the retroarc thrust belt, while creation of space in the mantle wedge due to foundering allows retroarc underthrusting, and thus the cycle, to begin again (Kay *et al*., 1994; DeCelles *et al*., 2009; Ducea *et al*., 2013).

Therefore, these types of tectonomagmatic feedback cycles, which typically last 25-80 Myr (Chapman *et al*., 2021), are driven in part by the formation and removal of an arclogitic root. Renewal of the Cordilleran cycle depends on the root reaching a density conducive to foundering into the mantle. Moreover, how fast these cycles occur is a function of arclogite removal rates, which are governed by the magnitude of the density contrast between the arclogitic lithosphere and underlying mantle (Jull & Kelemen, 2001; Valera *et al*., 2011; Krystopowicz & Currie, 2013; Currie *et al*., 2015). Using densities up to 3.6 g/cm^3, which represent a typical garnet- and clinopyroxene-bearing rock (Ducea, 2002; Lee *et al*., 2006; Jagoutz & Schmidt, 2013), numerical and geodynamic models predict root evacuation within 10 Myr of formation (e.g. Jull & Kelemen, 2001; Le Pourhiet *et al*., 2006; Krystopowicz & Currie, 2013; Currie *et al*., 2015; Lee & Anderson, 2015; Wang *et al*., 2015). Yet these models do not consider that the deep crustal hot zone of an active, thick-crusted Cordilleran arc is most likely a mush zone, where a framework of crystals coexists with partial melt (Hildreth & Moorbath, 1988; Annen *et al*., 2006; Huang *et al*., 2015; Delph *et al*., 2017). As such, felsic melt retained within the arclogitic residue may lower the density of the root, potentially so much so as to offset the negative buoyancy of the garnet pyroxenitic mass (Ducea *et al*., 2021a). The subarc root is also assumed by most conceptual (e.g. DeCelles *et al*., 2009) and geodynamic (e.g. Currie *et al*., 2015) models to be entirely composed of gravitationally unstable arclogite, yet partial melting of felsic to intermediate continental crust in the hot zone may not form arclogitic assemblages with densities suitable for foundering (Hacker *et al*., 2005; Patiño Douce, 2005). Here, we aim to address these model deficiencies by

first exploring how the presence of melt influences the foundering ability of a residual arclogitic root. Through phase equilibria modeling, we then investigate how crystallization of basaltic magma, partial melting of crustal lithologies, and melt accumulation and extraction in the lower crust of an active arc affect the density and mineralogical evolution of the residual root. We show that the presence of melt as well as the lithology of assimilated material in the hot zone greatly influence whether the residual root will founder into the underlying mantle.

THE DEEP CRUSTAL HOT ZONE OF CORDILLERAN ARCS: CHARACTERISTICS AND PETROGENETIC PROCESSES

At subduction zones, partial melting of both the downgoing, dehydrating oceanic crust and the water-fluxed, adiabatically decompressing mantle wedge produces hydrous mafic magmas that rise toward the surface (Davies & Stevenson, 1992). During ascent, these magmas intrude and stall within the lowermost continental crust at a point of neutral buoyancy (Thybo & Artemieva, 2013). Repeated underplating of hot basaltic magmas near the Moho displaces the steady-state geotherm to higher temperatures and generates partially molten regions in the lowermost crust of an active arc (Fig. 1b; Annen & Sparks, 2002; Dufek & Bergantz, 2005). These regions are referred to in this paper as deep crustal hot zones after Annen *et al*. (2006) and are analogous to the mixing, assimilation, storage, and hybridization zones of Hildreth & Moorbath (1988).

Within the hot zone, modification of mantle-derived melts as well as reworking of the surrounding crust (Dufek & Bergantz, 2005; Annen *et al*., 2006) generate the intermediate calc-alkaline magmas that typify Cordilleran arcs (Ducea *et al*., 2015). In particular, magmatic processing is achieved via two end-member mechanisms: (1) fractional crystallization of underplated mafic magma and (2) partial melting of previously intruded basaltic underplates as well as the surrounding lower crust (e.g. Jagoutz & Klein, 2018). In the latter case, because

primitive arc basalts have temperatures ranging between 1100-1300°C (Medard & Grove, 2008) and H_2O contents greater than ~10 wt.% (Grove *et al*., 2012), repeated influx of mafic magma into the subarc lower crust supplies the heat and fluids necessary to instigate melting of the country rock (Huppert & Sparks, 1988; Weinberg & Hasalová, 2015; Collins *et al*., 2016, 2020). Melt-rock interaction in the deep crustal hot zone, although beyond the scope of this paper, has also been shown to play a role in modifying melts and the crystal mush/country rock through which they flow (Daczko *et al*., 2016; Jackson *et al*., 2018).

It is debated as to which end-member mechanism – fractionation of mafic magmas or partial melting of the preexisting crust – is primarily responsible for the formation of intermediate to felsic arc magmas, especially during Cordilleran high-flux events (see Annen *et al*., 2015 and Jagoutz & Klein, 2018 for current reviews). Inefficient basalt-crust heat transfer may prevent significant contributions from wall rock assimilation (Dufek & Bergantz, 2005), except perhaps in the deepest crust where temperatures are already elevated (DePaolo, 1981). In contrast, temperatures within the hot zone are sufficiently high to permit extensive fractional crystallization (Annen *et al*., 2006). Evidence for differentiation of arc basalts in the deep crust include the low Dy/Yb as well as high Sr/Y and La/Yb ratios of arc magmas, indicating fractionation of amphibole and garnet, respectively (Davidson *et al*., 2007; Profeta *et al*., 2015), although these signatures may be inherited from mantle sources (Turner & Langmuir, 2015). Upper crustal batholiths also have geochemical signatures suggesting a genetic relationship with deep-seated, cumulate-textured xenoliths (Ducea & Saleeby, 1998; Lee *et al*., 2006) and exhumed lower crustal exposures (Kidder *et al*., 2003; Greene *et al*., 2006; Jagoutz & Schmidt, 2013; Bucholz *et al*., 2014; Walker *et al*., 2015). In addition, arc geochemistry plotted on Harker diagrams produce curvilinear differentiation trends, further bolstering the idea that felsic continental crust is derived from fractionation of basaltic magmas (Keller *et al*., 2015). Overall, if

fractionation acts alone, ~40-60% to >80% basalt crystallization is required to produce andesitic to rhyodacitic residual magmas, respectively (Müntener & Ulmer, 2006; Nandedkar *et al*., 2014).

Yet partial melting of the preexisting crust cannot be discounted as an important process of magma modification in the hot zone. Because they incorporate upper plate crust and mantle lithosphere, many Cordilleran batholiths and their residues contain inherited zircons (Murphy & Chapman, 2018) and display evolved, crustally contaminated Nd, Sr, Hf, and O isotopic compositions (Esperança *et al*., 1988; Smith *et al*., 1994; Ducea, 2002). In particular, arclogites from the Sierra Nevada have average whole-rock $\delta^{18}O = 7.5‰$ relative to SMOW, much higher than mantle compositions and indicative of metasediment assimilation (Ducea, 2002). Isotopic evidence also suggests ~50% of the mass of arc magmas generated during high-flux events along the North American Cordillera may be derived from lithosphere underthrust beneath the arc (Ducea & Barton, 2007).

Overall, fractionation and partial melting operate in tandem to generate large volumes of refractory cumulates and restites, respectively (Ducea & Saleeby, 1998; Ducea, 2002; Ducea *et al*., 2021a). These residues, which remain in the hot zone after melt extraction, accumulate to form the lower crustal and mantle lithospheric root of the arc. To satisfy mass balance, the mass of Cordilleran batholiths must be complemented by 1 to 3 times more residue in the arc root (Ducea, 2002). At thin (<35-40 km) arcs, cumulates and restites are granulites or pyroxenites dominated by plagioclase (Ducea *et al*., 2021a). At greater pressures (>1.2 GPa) consistent with the depth of Cordilleran lower crust (>35-40 km), fractionation and partial melting produce dense residual roots composed of garnet, clinopyroxene, amphibole, and Fe-Ti oxides (Ducea & Saleeby, 1996). Termed arclogites (Lee & Anderson, 2015), these residues are negatively buoyant and tend to founder into the mantle via Rayleigh-Taylor-type (RT) instabilities ("drips"; Houseman *et al*., 1981) or via delamination (Bird, 1979).

Arclogites are exposed within the lowermost crust of exhumed paleo-arcs. While the Talkeetna paleo-arc only retains 100-400 m of arclogitic rocks at the exposed Moho (Jagoutz & Kelemen, 2015), the Kohistan (Jagoutz & Schmidt, 2012; Jagoutz & Schmidt, 2013) and Fiordland (Hacker *et al*., 2008) crustal sections preserve 13 and 10 km (barometrically corrected thickness) of unfoundered, density-unstable garnet-bearing residues, respectively. What kept the negatively buoyant root of these arcs from foundering? One possibility is that the arc root at the time of tectonic obduction was partially molten. Temperatures of the orogenic lower crust approximated from thermometry of arclogite exposures (Esperança *et al*., 1988; Smith *et al*., 1994; Ducea & Saleeby, 1996; Ringuette *et al*., 1999; Weber *et al*., 2002; Yoshino & Okudaira, 2004; Lee *et al*., 2006; Dhuime *et al*., 2009; Gysi *et al*., 2011; Erdman *et al*., 2016; Rautela *et al*., 2020) and amphibolite/granulite terranes (Depine *et al*., 2008; Triantafyllou *et al*., 2018) range on average from 700-950^{o}C. This temperature range exceeds both the high-pressure water-saturated and water-absent solidi of typical lower crustal assemblages (Vielzeuf & Schmidt, 2001). Therefore, the arc root is likely to be a melt-bearing region, with melt extraction out of the hot zone balanced by influx of hot mantle-derived magma (Ducea *et al*., 2021a). The presence of trapped melt decreases the overall density of the residual root, potentially leading to neutral or positive buoyancy with respect to the mantle. Tassara (2006) estimated <8 vol.% andesitic melt must be retained within dry mafic granulitic lower crust at 1.5 GPa to achieve gravitational stability. Volumes of intermediate melt anywhere between 22-35% have been shown by Ducea *et al*. (2021a) to stabilize an arc root of arclogitic composition at 850^{o}C and 1.5 GPa.

Geophysical observations provide insight into the amount of melt present in the lower crust beneath active volcanic regions. The Yellowstone superplume is underlain by a lower crustal magma body interpreted from seismic data to contain ~2 vol.% melt (Huang *et al*., 2015). In a high-resolution seismic study of the central Andean Puna Plateau, Delph *et al*. (2017) use a

joint inversion of receiver functions and surface-wave dispersion data to reveal a >60 km-deep, near-Moho subarc hot zone with 4-9 vol.% melt. According to seismic (Ward *et al*., 2014; Delph *et al*., 2017; Koch *et al*., 2021) and magnetotelluric studies (Brasse *et al*., 2002; Schilling *et al*., 2006; Comeau *et al*., 2015; Comeau *et al*., 2016) in the Andes, deep-seated subarc magma reservoirs such as this feed mid-crustal (5-25 km depths) mush zones interpreted to contain melt volumes anywhere between 4-27%.

EFFECT OF RETAINED MELT ON THE FOUNDERING ABILITY OF RESIDUAL SUBARC ROOTS

Effect of retained melt on the density of residual subarc roots

First-order controls on the susceptibility of the subarc root to convective removal include the density and viscosity of the residual arclogite (Krystopowicz & Currie, 2013; Currie *et al*., 2015). For the arc root to founder via drip-like removal, it must have a density exceeding that of the underlying mantle (Jull & Kelemen, 2001). Such high densities characterize garnet ± amphibole-bearing clinopyroxenites at the temperature and pressure conditions of Cordilleran lower crust. However, within an active hot zone, low-density melt trapped within the arclogitic assemblage will reduce the root's negative buoyancy (Tassara, 2006; Ducea *et al*., 2021a). How much melt must be present to offset the density contrast between the arclogitic lower crust and the underlying mantle, thereby hindering convective removal of the subarc root?

To address this question, we envision a Cordilleran arc underlain by a lower crustal root composed of cumulate and restitic arclogite. In order to examine the effect of crustal thickness on the density of a melt-bearing root, we consider three Cordilleran arcs – a "thin" arc with a root at 1.5 GPa (50 km), a "thick" arc with a root down to 2 GPa (65 km), and a "very thick" arc with a root reaching pressures of 2.5 GPa (~80 km-thick crust). These scenarios correspond well with

the crustal structure beneath a range of active and ancient Cordilleran arcs. For example, the eastern Trans-Mexican Volcanic Belt is a "thin" arc with crustal thicknesses of 45-50 km (Ferrari *et al*., 2012). The Fiordland arc section extends to depths of at least 65 km (Klepeis *et al*., 2019), consistent with the thick arc scenario. Together, the thin and thick arc scenarios approximate crustal thicknesses beneath parts of the Western Cordillera-Puna Plateau (McGlashen *et al*., 2008), portions of the northern Andean Ecuadorian arc (Koch *et al*., 2021), and encompass the range of crustal thickness values estimated for the Arizonaplano and Nevadaplano retroarc plateaus of the North American Cordillera (Chapman *et al*., 2015; Chapman *et al*., 2020). The very thick arc scenario resembles the crustal structure beneath parts of the Western Cordillera-Altiplano Plateau in the central Andes (Beck *et al*., 1996; McGlashan, 2008; Ryan *et al*., 2016). While active, the ancient Sierra Nevada and Coast Mountains arcs fluctuated between all three scenarios (Profeta *et al*., 2015).

In our models, for the thick and very thick arc scenarios, the arc root is composed of arclogite with 50 vol.% group B garnet (almandine, grossular, and pyrope in equal proportions) and 50 vol.% diopsidic clinopyroxene (Ducea *et al*., 2021a). In the thin arc case, the arc root consists of equal parts group B garnet and diopsidic clinopyroxene as well as 10 vol.% pargasitic amphibole. To investigate the effect of entrained melt on the density of the root, we assume that the hot zone comprises 0-30 vol.% hydrous tonalitic/granodioritic melt with a chemical composition equal to that of an average North American Cordilleran batholith (Ducea *et al*., 2015) + 10 wt.% H_2O (Grove *et al*., 2012). Melt in our models is regarded as equally distributed throughout the subarc root. At the specified pressure conditions for temperatures ranging between 600-1200^{o}C, we calculate the density of the melt after Bottinga & Weil (1970), Lange & Carmichael (1987), and Kress & Carmichael (1991) as well as the density of the solid arclogitic assemblage following Abers & Hacker (2016). The density of the melt-bearing root is then

determined by summing the densities of the arclogite and the melt according to their proportions in the hot zone.

Figure 2 shows that the addition of 5 vol.% melt decreases the density of the arc root by 0.05 g/cm^3 for all pressures. For temperatures consistent with the subarc lower crust (700-950^{o}C), this means that roots reaching pressures of 1.5, 2, and 2.5 GPa (equivalent to depths of ~50, 65, and 80 km) require at least 10, 15, and 18 vol.% melt, respectively, to achieve a density neutral with that of the upper mantle. It is important to note that in this paper, we treat RT-type instabilities as the primary mechanism of foundering/removal (Houseman *et al*., 1981; Conrad, 2000; Saleeby *et al*., 2003). This is because geodynamic models indicate a strong likelihood of RT-type lithospheric removal in Cordilleran orogens (Currie *et al*., 2015), which is affirmed by the presence of drip-induced "bobber basins" (Fig. 1a; DeCelles *et al*., 2015b) as well as seismic images of descending blobs (Beck & Zandt, 2002; Zandt *et al*., 2004). RT-type dripping is also simpler to model, as it does not necessitate the development of a mechanically weak zone (Meissner & Mooney, 1998). Because foundering via RT instability commences when the arc root reaches a density 0.05 g/cm^3 greater than that of the underlying mantle (Currie *et al*., 2015), we posit that an arclogitic root comprising >10-18 vol.% hydrous intermediate melt is gravitationally stable in the lowermost part of 50-80 km-thick crust.

Effect of retained melt on the rate of subarc root removal

Based on the above results, a residual subarc root with 0-10 vol.% intermediate melt still has a density conducive to foundering at all modeled pressures, although the density contrast between the root and underlying mantle is reduced. Geodynamic and numerical models have found that the smaller the density contrast between the arc root and the upper mantle, the slower the removal (Jull & Kelemen, 2001; Valera *et al*., 2011; Krystopowicz & Currie, 2013; Currie *et al*., 2015).

But the addition of only 1-7 vol.% melt also significantly decreases the aggregate strength of the continental crust, with 7 vol.% melt causing a ~90% strength reduction (Rosenberg & Handy, 2005). The presence of melt therefore facilitates lithospheric removal (Krystopowicz & Currie, 2013; Currie *et al*., 2015). Given these considerations, how does the presence of small amounts of partial melt affect the rate of foundering?

The rate at which the arclogitic root detaches via RT-type dripping can be expressed mathematically as

$$t_{crit} \sim \frac{\eta_x}{\Delta\rho_x g H} \quad (1)$$

where the time for foundering (t_{crit}) is related by an order of magnitude approximation to the viscosity of the arclogitic root (η_x), the density contrast between the root and underlying mantle ($\Delta\rho_x$), the thickness of the root (H), and gravity (g) (Lee, 2014). Clearly, the denser, thicker, less viscous the subarc root, the greater the rate of foundering. We first envision a 10-km-thick solid arclogitic root at 850°C and 2 GPa. The density of this root at these conditions according to Figure 2 is 3.52 g/cm^3. Assuming an average mantle density of 3.3 g/cm^3, $\Delta\rho_x$ = 0.22 g/cm^3. The parameter η_x is more difficult to constrain because the rheology of garnet- and diopside-bearing arclogites has yet to be studied. Nevertheless, flow laws exist for omphacite-bearing dry eclogite (Jin *et al*., 2001; Zhang & Green, 2007). We use viscosities of 10^{21} and 10^{22} Pa·s for a dry eclogite at a strain rate of 10^{-15} s^{-1} and a temperature of ~850°C, viscosities of which approximate the range of plausible root viscosities modeled by Currie *et al*. (2015). Inputting these parameters into Equation 1 yields a solid arclogitic root that will founder within 1 to 15 Myr. This is consistent with previous estimates from modeling efforts of <10 Myr for complete root removal (Jull & Kelemen, 2001; Le Pourhiet *et al*., 2006; Krystopowicz & Currie, 2013; Currie *et al*., 2015; Lee & Anderson, 2015; Wang et al., 2015). Evidence of drip-induced surface deflection

and deformation in the central Andean plateau indicates lithospheric removal within ~2-7 Myr, also congruent with our results (DeCelles *et al*., 2015b; Schoenbohm & Carrapa, 2015). We must keep in mind, however, that arclogites may be inherently more viscous than eclogites owing to the absence of the weak minerals omphacite and phengite and the greater proportion of the strong mineral garnet (Shea & Kronenberg, 1993; Jin *et al*., 2001; Zhang & Green, 2007), and this may cause arclogites to founder at rates slower than our computations suggest.

To calculate the effect of partial melt on the time for foundering, we consider an arclogitic root with 5 vol.% melt, consistent with geophysical estimates of melt fractions in the subarc lower crust (Delph *et al*., 2017). This melt percentage corresponds to a root density of 3.47 g/cm^3 and $\Delta\rho_x$ of 0.17 g/cm^3 (Fig. 2). The viscosity of the melt-bearing root is greatly affected by the addition of melt, which causes dramatic weakening of crustal rocks (Rosenberg & Handy, 2005; Rosenberg *et al*., 2007). Based on the flow law of Paterson (2001), a melt volume of just 5% decreases the viscosity of a mafic rock by around an order of magnitude. This yields $\eta_x = 10^{20}$-10^{21} Pa·s if all other variables remain unchanged. Using Equation 1, we calculate the time for foundering of a melt-bearing root to be 200 Kyr to 2 Myr – an order of magnitude faster removal than that for a solid root. This range of timescales is corroborated by numerical and geodynamic models of lithospheric removal, which suggest that a rheologically weak root can under appropriate conditions founder within ≤1 Myr (Currie *et al*., 2015; Lee & Anderson, 2015). Currently, there are no published studies citing geologic evidence for foundering at Kyr timescales. Geologic evidence of dripping that provides insight into the timescales of foundering includes the surface subsidence that occurs during drip formation as well as the rapid uplift that ensues after drip detachment (e.g. Göğüş & Pysklywec, 2008; DeCelles et al., 2015b; Schoenbohm & Carrapa, 2015). However, if the lower crust is weak, crustal flow above the

descending instability causes crustal thickening (Elkins-Tanton, 2007; Krystopowicz & Currie, 2013; Currie *et al*., 2015; Wang *et al*., 2015), which can either counteract surface subsidence related to root formation, resulting in minimal surface deflection, or cause uplift rather than subsidence as the root develops (Wang *et al*., 2015). Furthermore, more rapid foundering results in smaller magnitude surface deflections (Wang *et al*., 2015). As such, in regions of thick crust weakened by high temperatures and the presence of melt, like the frontal Cordilleran arc, Kyr-scale foundering events may not be detected from geologic evidence.

In summary, our results indicate that when melt in the hot zone is present in volumes <10-18%, which is probable according to geophysical evidence, the substantial melt-driven drop in viscosity promotes rapid foundering of the arclogitic lithosphere. Interestingly, because arclogites with up to 10 vol.% melt form dense, low-viscosity roots, their swift removal may serve to transfer hydrous, high-SiO_2, incompatible element-rich melt into the mantle. The addition of >10-18 vol.% melt, on the other hand, decreases density so much so as to offset the negative buoyancy of the arclogite, thereby preventing root removal via RT instability. It is not until after complete or partial melt extraction that the arclogitic keel, now with <10-18 vol.% melt, becomes negatively buoyant such that it can founder (Ducea *et al*., 2021a). Thus, the influence of trapped melt on the density and viscosity of arclogite is an important effect to consider when modeling gravitational foundering of magmatic arc roots.

The first-order calculations performed above arbitrarily add felsic melt to a gravitationally unstable arclogitic root without acknowledging 1) phase stability at different temperatures, pressures, and water contents and 2) processes that occur within a dynamic hot zone, such as partial melting and crystallization. In the next section, we conduct open-system thermodynamic modeling to constrain the density evolution and foundering ability of restites and cumulates in equilibrium with their derivative melts.

PHASE EQUILIBRIA MODELING

Theory

Within the hot zone, partial melting of crustal lithologies occurs contemporaneously with crystallization of underplated basalts (Fig. 1b). We use the Gibbs free-energy minimization software Perple_X (Connolly, 2005, 2009), the thermodynamic dataset of Holland & Powell (2011), and internally consistent sets of thermodynamic solution models (White *et al*., 2014; Green *et al*., 2016) to investigate how the mineralogy and density of cumulates and restites in equilibrium with their derivative melts evolve during crystallization and partial melting and affect the foundering ability of the subarc root. Because many solution models are not calibrated for high pressures (>2 GPa), we model partial melting and crystallization only at 1.5 GPa ("thin" arc) and 2 GPa ("thick" arc) for temperatures between 600-1100^{o}C.

We assume that within the deep crustal hot zone, mantle-derived basalts intrude three different end-member lithologies: (1) pre-existing mafic amphibolite or previously underplated metabasalt, (2) metapelite, and (3) metagraywacke. In response to elevated temperatures and/or an influx of fluids, these rocks undergo partial melting, generating felsic magma and solid restites as temperatures increase.

When melting occurs, the melt distribution will be controlled by the propensity of the system to minimize interfacial energy (Watson, 1982; McKenzie, 1984). Melt will wet grain boundaries if the melt-crystal interfacial energy is lower than the crystal-crystal interfacial energy. If larger, melt will pool. This effect is described by the dihedral angle, which determines the interconnectivity of the melt phase. For an isotropic system, dihedral angles ≤60^{o} allow full interconnectivity of melt channels along grain edges, even at incredibly small melt volumes (<1%). If the dihedral angle is >60^{o}, melt is isolated at 4-grain corners. However, minerals like

clinopyroxene and amphibole display surface energy anisotropy that results in a more complex melt geometry. To characterize the melt geometry in natural anisotropic systems, Holness (2006) measured the equilibrium melt-solid dihedral angles of quartz, plagioclase, amphibole, and clinopyroxene within basaltic, andesitic, and rhyolitic compositions. She found that quartz and plagioclase have melt-solid dihedral angles $<30^{o}$, while amphibole and clinopyroxene have dihedral angles of $28^{o} \pm 14.4^{o}$ and $37\text{-}39^{o} \pm 13\text{-}15^{o}$. We can therefore make the simplifying assumption that for the geologic systems modeled here, the equilibrium melt-solid dihedral angle is $<60^{o}$ (McKenzie, 1984; Holness & Sawyer, 2008). For an anisotropic rock, this means that the melt will form an interconnected network at some melt fraction threshold. It is at this threshold that melt is able to drain from the system (e.g. Sawyer, 1994; Petford, 1995; Bons *et al*., 2004; Brown, 2004). Once this melt volume is achieved and melt loss occurs, further heating and melt build-up to the threshold result in additional melt extraction events. We therefore treat melt accumulation and subsequent melt loss as a cyclic process (Handy *et al*., 2001; Bons *et al*., 2004; Rabinowicz & Vigneresse, 2004; Brown, 2007), occurring repeatedly as temperatures rise until the residue is no longer melt-fertile.

Estimates of the melt volume at which an extractable interconnected network of melt is established are typically less than 10% (Bons *et al*., 2004; Clemens & Stevens, 2016). For example, experimental studies on quartzite (Laporte *et al*., 1997) and amphibolite (Wolf & Wyllie, 1991; Lupulescu & Watson, 1999) report melt interconnectivity and segregation at <0.04 vol.% and 2-5 vol.% melt, respectively. Numerical models of granitic melt segregation from the middle to lower continental crust suggest a threshold value of 5 vol.% melt (Rabinowicz & Vigneresse, 2004). Similarly, Vigneresse *et al*. (1996) argue that a continuous melt network is achieved at 8 vol.% melt for partially molten gneiss. In their seminal study on the rheology of melting rocks, Rosenberg & Handy (2005) compiled experimental data on the aggregate strengths

of partially melted crustal rocks undergoing deformation at low shear strains. They show that as the volume of melt grows from 0 to 7%, the proportion of melt-bearing grain boundaries rapidly increases from 0 to >80%, thus forming an interconnected network of melt. The attainment of 7 vol.% melt defines the melt connectivity transition (MCT) – the fraction of melt necessary to induce a rapid strength drop in melt-bearing rocks as deformation transitions from intragranular to intergranular (Rosenberg & Handy, 2005). Because this transition marks the point by which melt becomes interconnected, it is at the MCT that a number of workers expect melt extraction from crustal rocks to occur (e.g. Rosenberg & Handy, 2005; Brown, 2007; Rosenberg *et al*., 2007; Korhonen *et al*., 2010; Yakymchuk & Brown, 2014; Diener & Fagereng, 2014; Palin *et al*., 2016). Melt extraction at or before the MCT is especially likely under intense deformation. The observation that leucosomes collect within low-pressure sites is evidence that small volumes of melt can segregate readily from the residue during deformation and undergo potential melt loss (Sawyer, 1991; Brown, 1994). This is because high strain rates induced by syn-anatectic deformation, a likely scenario in the deep Cordilleran crust (Kidder *et al*., 2003), facilitate more rapid melt migration by establishing pressure gradients, allowing the formation of an interconnected network at melt volumes as low as 1% (Sawyer, 1991, 1994; Brown, 1994; Rosenberg & Handy, 2001; Handy *et al*., 2001; Bons *et al*., 2004). However, the distribution of strain in the orogenic lower crust, as well as the magnitude of the deformation-assisted melt fraction threshold in these settings, are unknown.

Methods

Because Cordilleran orogens are dynamic systems, we view the MCT as a reasonable maximum threshold for melt extraction (Brown, 2007; Diener & Fagereng, 2014; Yakymchuk & Brown, 2014; Palin *et al*., 2016). This is consistent with the amount of melt (2-9 vol.%) imaged within

the lower crust beneath active volcanic regions (Huang *et al*., 2015; Delph *et al*., 2017). We therefore simulate open-system behavior in our partial melting models by adopting the approach of Palin *et al*. (2016) and extracting melt as soon as 7 vol.% is produced. Because granulites and migmatites often record microstructures, such as melt pseudomorphs (e.g. Holness & Sawyer, 2008), that indicate the retention of small melt volumes (<2%), we assume incomplete melt extraction such that 1 vol.% melt remains trapped in the residue after each melt loss event (Sawyer, 2001; Brown, 2010; Yakymchuk & Brown, 2014; Palin *et al*., 2016). This agrees with McKenzie (1984)'s estimate of <3 vol.% retained melt derived from numerical methods.

Following melt evacuation, the composition of the partially melted residue is calculated and becomes the starting composition for the subsequent model. In this way, assuming temperatures rise steadily following injection of basaltic magma into the hot zone, we model partial melting and successive melt extraction until the residue can no longer generate 7 vol.% melt at temperatures between 600-1100°C. We refer to this infertile residue as melt-depleted.

To simulate assimilation of pre-existing mafic amphibolite or solidified basaltic underplates, we model partial melting of an average hydrous primitive basalt from the Kamchatka arc (Table 1; Schmidt & Jagoutz, 2017) in the Na_2O-CaO-FeO-MgO-Al_2O_3-SiO_2-H_2O-TiO_2 system (see Appendix A for solution model information). Because Perple_X generates pressure *vs.* temperature pseudosections that can be viewed as depicting up-temperature batch melting or down-temperature batch crystallization, we use the initial models from our partial melting simulations to investigate the density and mineralogy of cumulates as they crystallize in the lower crust. Models assume underplated basalts undergo batch crystallization at a single depth within the hot zone until the residual melt reaches conditions such that it can buoyantly rise. We do not model fractional crystallization, a polybaric process that continues to operate even after the residual magma has departed the hot zone.

We also model partial melting of metasedimentary country rock including metapelite (mature clastic sediment) and metagraywacke (immature clastic sediment), which are commonly found in orogenic terranes as former passive margin sequences. For our metapelite starting composition, we use an average amphibolite facies metapelite from Ague (1991) (Table 1). The composition of the metagraywacke is taken as that of sample ES356 from Sawyer (1986), a peraluminous (molar ratio of $Al_2O_3/(CaO + Na_2O + K_2O) > 1$) rock compatible with the compositional restrictions on the metapelite solution models (Appendix A; White *et al*., 2014). We model both compositions in the Na_2O-CaO-K_2O-FeO-MgO-Al_2O_3-SiO_2-H_2O-TiO_2-O system with $Fe^{3+}/(Fe^{2+}+Fe^{3+}) = 0.15$ (White *et al*., 2014).

For both the metabasalt and metasedimentary models, we include in the bulk composition chemical components such as TiO_2 and O_2 that are not incorporated in the accompanying melt solution models. This approach is required to improve the stability of critical phases: the addition of TiO_2 in metabasalt models stabilizes Fe-Ti oxides and amphibole, while the inclusion of TiO_2 and O_2 in metasedimentary models improves the stability of Fe-Ti oxides and biotite. Although incremental melt extraction artificially enriches the residue in these components, this enrichment does not result in unrealistic phase equilibria. Finally, we model only fluid-absent melting for all compositions: our modeled compositions have water contents within 0.1 wt.% of the maximum amount of internally bound H_2O that can be contained within the rock at each pressure. Although we recognize flux melting as an important process in deep crustal hot zones, we mostly refrain from modeling fluid-saturated compositions because (1) Perple_X does not accurately reproduce the fluid-saturated solidus of metabasalts at the pressures of interest nor does it output a reasonable fluid-saturated solidus for metapelite and metagraywacke at 2 GPa and (2) fluid-saturated compositions undergo comparatively more melt extraction events, driving the residue to compositions for which existing solution models are not calibrated.

Results

Crystallization and partial melting of basalt

Figure 3 shows the phase equilibria for a primitive arc basalt from 600-1100°C at 1.5 and 2 GPa. Phases include amphibole, garnet, clinopyroxene, quartz, rutile, and plagioclase, the latter of which is only stable in the 1.5 GPa case. We first consider batch crystallization of mantle-derived basaltic underplates in the hot zone. By 1100°C, the magma has undergone 60-70% crystallization. Cumulates at this temperature are dense (>3.45 g/cm^3) arclogites with near-equal proportions of garnet and clinopyroxene. Arclogitic cumulates at 1.5 GPa further contain ~5 vol.% amphibole, consistent with experimental results (Wyllie & Wolf, 1993; Sen & Dunn, 1994). Cumulates maintain high densities until greater than ~10 vol.% amphibole crystallizes. Phase proportions at this point depart from the mineralogy of an average arclogite (Ducea *et al*., 2021a) as amphibole becomes a dominant phase in the crystallizing rock, causing the density of the residue to decrease dramatically as temperatures drop. At 1.5 GPa, >80% crystallization is required for the residue to become gravitationally stable. In contrast, >95% crystallization must occur for residue at 2 GPa to attain a density below 3.35 g/cm^3. Although near-complete crystallization of basaltic underplates is likely in the cold lower crust of a nascent Cordilleran arc (Jackson *et al*., 2018), basalts intruded into long-lived hot zones only undergo fractionation until extraction of the residual melt can occur. Because upper crustal tonalitic/granodioritic batholiths have been shown to form after ~40-60% crystallization of mafic magma (Müntener & Ulmer, 2006; Nandedkar *et al*., 2014), it is likely that the majority of cumulates that form in the lower crust are density unstable and susceptible to foundering (Fig. 4a). However, it is clear from Figure 3 that cumulates coexisting with their residual melts maintain densities equal to or lower than that of the mantle within the modeled temperature range. Thus, as long as melt extraction

does not occur during crystallization, the fractionating assemblage cannot develop negative buoyancy with respect to the mantle. Although we model only at water-undersaturated conditions, if we assume melt extraction occurs prior to >80% crystallization, our modeled cumulates achieve densities (3.35-3.52 g/cm^3) similar to those of average arclogite (~3.4-3.55 g/cm^3; Ducea, 2002; Jagoutz & Schmidt, 2013) (Fig. 5).

We can also view Figure 3 as the closed-system prograde evolution of a solidified metabasaltic underplate or lower crustal amphibolite. At 700°C, the metabasic rock has a density equal to or lower than that of the mantle and is gravitationally stable in the lower crust. An influx of hot mafic magma, for example, drives isobaric heating within the hot zone, causing amphibole dehydration and melt generation at ~800°C. Incongruent breakdown of amphibole yields garnet, clinopyroxene, and melt (Rapp *et al*., 1991; Wolf & Wyllie, 1993; Wyllie & Wolf, 1993; Sen & Dunn, 1994; Wolf & Wyllie, 1994; Rapp & Watson, 1995; Vielzeuf & Schmidt, 2001). Consistent with dehydration melting experiments on amphibolite (Wyllie & Wolf, 1993; Sen & Dunn, 1994), amphibole is fully consumed by ~900°C at 2 GPa but persists to higher temperatures at 1.5 GPa. As melting continues, the density of the residue at 2 and 1.5 GPa increases steadily, exceeding that of the mantle by 850 and 920°C, respectively; however, in the absence of melt extraction, the melt-bearing residue remains gravitationally stable at all suprasolidus temperatures.

Because large amounts of melt are not rheologically stable in the lower crust, we model open-system partial melting within arc roots at 1.5 and 2 GPa by invoking episodic melt extraction at the MCT (Fig. 6). Our models show that, compared to closed-system behavior, repeated melt loss substantially impacts the mineralogy and density evolution of the metabasaltic assemblage as well as the susceptibility of the assemblage to foundering. This is because cyclic melt extraction generates bulk compositions that become progressively denser, less hydrous, and

more chemically depleted as temperatures increase and the residue melts. At 1.5 GPa and <800°C, the subsolidus metabasalt contains amphibole, clinopyroxene, garnet, quartz, and minor rutile and is gravitationally stable in the lower crust (Fig. 6a). Our models assume that once partial melting commences, the rock is always in equilibrium with 0-7 vol.% melt until the final melt extraction event yields an infertile residue. Increasing temperatures steadily from 800-1100°C at 1.5 GPa generates a melt-bearing residue that maintains a density lower than or equal to that of the mantle until the third and final melt extraction event at ~940°C. At this point, melt escapes the system and leaves behind melt-depleted restite that can no longer generate 7 vol.% melt within the modeled temperature range (Fig. 6a, b). With densities >3.4 g/cm^3, this restite is capable of foundering into the mantle. Significantly, this melt-depleted density-unstable residue is hydrous, being composed of ~10 vol.% amphibole as well as near-equal proportions of garnet and clinopyroxene with minor plagioclase (<5 vol.%) and rutile (<1 vol.%).

We note that although amphibole-out at 1.5 GPa is >50°C higher in our models (>1100°C) than experiments indicate (~1050°C; Wyllie & Wolf, 1993; Sen & Dunn, 1994; Rapp & Watson, 1995; Müntener *et al*., 2001), the presence of amphibole at these temperatures is plausible for several reasons. First, the lower water content (0.19 wt.%) of the modeled residue compared to experimental samples likely elevates the upper temperature limit of amphibole (e.g. Green *et al*., 2014; Mandler & Grove, 2016). Progressive loss of 7 vol.% melt has also been shown to enhance the stability of amphibole to higher temperatures (Palin *et al*., 2016). Finally, there are amphibole-rich lower crustal xenoliths that record peak temperatures greater than those experimentally determined for amphibole-out. For example, amphibole-bearing arclogites from the Mercederes region of the Colombian Andes and the Jijal sequence of the Kohistan paleo-arc record temperatures between 1073-1134°C at pressures of 1.9-2.1 GPa (Ringuette *et al*., 1999;

Bloch *et al*., 2017), more than 150°C greater than the experimentally determined amphibole-out (~900°C at 2 GPa).

At arc roots reaching depths corresponding to pressures of 2 GPa (Fig. 6c), subsolidus mafic assemblages consist of amphibole, clinopyroxene, garnet, quartz, and rutile and have densities within the range of upper mantle. Once partial melting begins, melt extraction at 870°C generates a residue that, even in the presence of up to 7 vol.% melt, maintains a density >3.4 g/cm^3. This garnet pyroxenitic residue, not yet melt-depleted, remains hydrous until amphibole is exhausted at 900°C. The second and final melt extraction event occurs at 975°C and leaves behind a dense (>3.45 g/cm^3), anhydrous (amphibole-absent) residue consisting of garnet and clinopyroxene in near-equal proportions as well as minor quartz (<3 vol.%) and rutile (<1 vol.%).

Significant similarities and differences exist between restites formed from basaltic protoliths at 1.5 and 2 GPa. At both pressures, melt-depleted residues will founder into the mantle (Fig. 4a), having mineralogies and densities that mirror those of an average arclogite (Fig. 5; Ducea *et al*., 2021a). This lends confidence to the validity of our models in simulating open-system partial melting in the deep lower crust. In addition, in contrast to the 1.5 GPa scenario, restites formed from partial melting of basaltic compositions at 2 GPa attain densities conducive to foundering prior to complete melt depletion. This means that in thicker arcs, restites can sink in the presence of hydrous melt, leading to accelerated foundering of the residual material. Furthermore, melt-depleted, density-unstable restite at 1.5 GPa contains amphibole within the modeled temperature range. In contrast, at 2 GPa, amphibole is only present within density-unstable restite from 870-900°C, being completely consumed prior to melt-depletion. Based on our results, we can infer that (1) lithospheric removal may transport hydrous, geochemically enriched felsic melt into the mantle, a process more likely to occur at thicker arcs (2 GPa) and (2)

amphibole-bearing arc roots, more likely at thinner arcs (1.5 GPa), can return fluids back into the mantle wedge as they sink to great depths.

Partial melting of metasedimentary country rock

The hot zone of an active arc contains metasedimentary rocks such as metapelites and metagraywackes (Kidder *et al*., 2003; Otamendi *et al*., 2009; Chin *et al*., 2013). These rocks, which can form the foundation upon which a Cordilleran arc is assembled, may also be transported into the subarc region via retroarc underthrusting (DeCelles *et al*., 2009) and/or relamination (Fig. 4b; Hacker *et al*., 2011). Trench-side sediments representing accretionary wedges or truncated forearcs may also be delivered to the subarc lower crust through underplating during flat slab subduction (Fig. 4b; Ducea & Chapman, 2018). Figures 7-8 depict the phase equilibria and densities of partially melted metapelite and metagraywacke subject to stepwise melt extraction at 1.5 and 2 GPa. At 1.5 GPa, subsolidus metapelite comprises white mica, garnet, quartz, clinopyroxene, Fe-Ti oxides, and biotite (Fig. 7a). Metapelite at 2 GPa includes the above phases, excepting biotite, plus volumetrically minor amphibole and kyanite (Fig. 7c). Similar subsolidus phase assemblages occur in metagraywackes, which contain white mica, garnet, clinopyroxene, quartz, and minor rutile, as well as biotite at 1.5 GPa and amphibole at 2 GPa (Fig. 8a, c). As temperatures rise and melting commences, alkali feldspar, aluminosilicates, garnet, and melt increase in proportion at the expense of hydrous phases, such as white mica, biotite, and amphibole, as well as clinopyroxene and quartz (Fig. 7-8). For both compositions, the breakdown of hydrous phases at 2 GPa produces melt at ~800-825^{o}C (Fig. 7c, 8c), in agreement with experimental constraints (Vielzeuf & Holloway, 1988; Vielzeuf & Schmidt, 2001). In contrast, metasedimentary rocks at 1.5 GPa cross the solidus as early as ~675-700^{o}C – a temperature range >150^{o}C lower than the fluid-absent solidus determined

experimentally at this pressure (Fig. 7a, 8a). Perple_X also ascribes the amphibolite-eclogite transition (i.e., biotite-out/clinopyroxene-in) to pressures lower than that identified in partial melting experiments (~2.1 GPa; e.g. Auzanneau *et al*., 2006). Because of these errors, we highlight only the most first-order results of these models.

Following melt depletion, metasedimentary residues are comprised of alkali feldspar (sanidine in metapelite, sanidine to anorthoclase in metagraywacke), garnet, an aluminosilicate polymorph, quartz, minor rutile, and at low temperatures, clinopyroxene (Fig. 7-8), similar to restites formed in partial melting experiments (Vielzeuf & Holloway, 1988; Patiño Douce & Beard, 1995; Patiño Douce & Harris, 1998; Patiño Douce & McCarthy, 1998; Vielzeuf & Schmidt, 2001; Auzanneau *et al*., 2006). Metapelitic restites at 1.5 GPa also contain small amounts of hydrous minerals, such as white mica and biotite, that break down at higher temperatures to form small-degree (<7 vol.%) melts (Fig. 7b). Significantly, it is evident from Figures 7-8 that at all modeled temperatures and pressures, open-system partial melting of metapelite and metagraywacke produces residues that are gravitationally stable within the lower crustal hot zone. With densities less than 3.25 g/cm^3, metasedimentary restites are incapable of foundering (Fig. 4-5).

Metasedimentary restitic xenoliths have been identified in nature (e.g. Schmid & Wood, 1976; White *et al*., 1999; Otamendi & Patiño Douce, 2001; Guernina & Sawyer, 2003; Hacker *et al*., 2005; Chin *et al.,* 2013; Morfin *et al*., 2013; Redler *et al*., 2013). One example of metasedimentary restites with mineralogies (alkali feldspar + garnet + quartz + aluminosilicate + rutile ± clinopyroxene) and densities (<3.25 g/cm^3) similar to our models are the sanidine eclogite xenoliths from the southern Pamir (Hacker *et al*., 2005). These xenoliths, which contain garnet, clinopyroxene, sanidine, kyanite, quartz, and rutile, equilibrated at pressures of 2.5-2.8 GPa and temperatures between 1000-1100^{o}C and are interpreted to be products of dehydration

melting of crustal metapelites. Significantly, these eclogites are positively buoyant with respect to the upper mantle, with densities ranging from 2.9 to 3.17 g/cm^3 (Fig. 5). This is in good agreement with our models, which at 2 GPa and 1100°C yield densities of ~3.15 g/cm^3 for melt-depleted metapelitic restites and ~2.9 g/cm^3 for the metagraywacke equivalent.

In contrast, lower crustal xenoliths and many of the lowermost zones of exhumed crustal sections are predominantly composed of mafic arclogites rich in garnet, pyroxene, and amphibole (e.g. Jagoutz & Schmidt, 2013). Only a few studies have provided evidence that metasediments are present in the subarc lower crust (Dodge *et al*., 1988; Ducea & Saleeby, 1996; Kidder *et al.*, 2003; Otamendi *et al*., 2009; Chin *et al*., 2013). Yet several processes proposed to occur at Cordilleran margins serve to transport melt-fertile metasediments into the hot zone. First, sediment underplating (Ducea & Chapman, 2018) and relamination of subducted sediments (Hacker *et al*., 2011) form felsic lower crust that can be remelted by arc magmatism (Fig. 4b). Second, based on isotopic evidence from arc magmas (Ducea & Barton, 2007), the Cordilleran cycle model (DeCelles *et al*., 2009) emphasizes melting of underthrust crust, at least 14-43% of which may be sedimentary in origin (Hacker *et al*., 2011). According to this model, crustal anatexis generates density-unstable arclogitic residues that founder into the mantle. This is in stark contrast to the low-density alkali feldspar-rich restites that are produced by our models and expected to form during partial melting of the metasedimentary portion of underthrust crust. If underthrust crust is predominantly tonalitic, dehydration melting is still expected to generate density-stable sanidine-bearing residues at temperatures <1050°C (Fig. 5; Hacker *et al*., 2005; Patiño Douce, 2005).

To further investigate whether partial melting of metasedimentary rocks can produce density-unstable arclogitic assemblages that help drive the Cordilleran cycle, we consider two

additional melting scenarios: 1) incremental melt extraction at 25 vol.% melt and 2) fluid-flux melting of metasedimentary lithologies (see Appendix B for details). In both cases, alkali feldspar is a major residual phase, and the restite remains positively buoyant with respect to the mantle at all modeled temperatures and pressures (Supplementary Fig. S1).

In summary, melting of metasediments coupled with incremental melt extraction at pressures between 1.5-2 GPa and temperatures up to 1100°C generates alkali feldspar-bearing residues with densities too low for foundering to occur (Fig. 5). Of course, our phase equilibria modeling results are limited by the chemical system, the pressure and temperature range of modeling, and the data available on the thermodynamic properties of minerals and melts (e.g. White *et al*., 2011). For example, we are limited by metapelite solution models to peraluminous compositions (White *et al*., 2014). To investigate the foundering ability of restites derived from metaluminous sediments, we calculated the density of restites experimentally produced by Patiño Douce & Beard (1995) from partial melting of quartz amphibolite. At 1.5 GPa and 950-1000°C, these restites have densities between 3.1-3.2 g/cm^3 and are stable in the lower crust. Furthermore, we only consider in this study three representative compositions of typical crustal rocks. According to partial melting experiments at 1.5 GPa, more Ti-rich, Al-poor metagraywacke forms gravitationally stable (2.87-3.06 g/cm^3; Patiño Douce & Beard, 1995; Auzanneau *et al*., 2006) residues as biotite breaks down to form peritectic garnet ± clinopyroxene ± orthopyroxene ± potassium feldspar (Fig. 5); once biotite is entirely consumed at 975°C, however, the residue can become density unstable under batch melting conditions (Patiño Douce & Beard, 1995). Partial melting at pressures greater than 2 GPa may also result in gravitationally unstable assemblages. For example, although most tonalitic restites are density-stable at pressures ≤2 GPa, pressures >2 GPa may yield negatively buoyant restites if melted at sufficiently high temperatures (Patiño Douce, 2005). Further studies are therefore necessary to fully determine the

fate of residues formed during open-system melting of typical crustal rocks beneath thick-crusted Cordilleran arcs.

DISCUSSION

The results of our calculations and models, the latter of which are summarized in Figures 4-5, are pertinent for the petrogenetic and tectonic processes that occur at Cordilleran arcs. Below we discuss the relevance of our results to the formation, preservation, and foundering of residues into the underlying mantle and the implications they have for the Cordilleran cycle model.

Preservation of residues in the hot zone

In exposed paleo-arcs such as Kohistan and Fiordland, thick sections of gravitationally unstable lithologies, including arclogites, are preserved in the lowermost crust. According to our results, stabilization of this dense lower crustal root may be aided by the presence of >10 vol.% low-density intermediate melt. In fact, following the India-Kohistan-Eurasia collision by 40 Ma (Martin *et al*., 2020), magmatism continued to supply the Kohistan batholith for an additional 10 Myr (Jagoutz *et al*., 2009). It is thus likely that prolonged melt in the lower crust of the Kohistan arc provided the positive buoyancy necessary to conserve the arc root.

Effect of the preservation of residues on surface elevation

We also address in this paper the extent to which crystallization and partial melting in the hot zone can produce density-unstable assemblages. According to our thermodynamic models, arclogite cumulates derived from fractionating basalts have densities exceeding the range of upper mantle and are thus prime candidates for foundering (Fig. 4a, 5). Basaltic rocks undergoing partial melting at 2 GPa attain similarly high densities after extraction of just 7 vol.% melt at

875°C. In comparison, at 1.5 GPa, residues of partially melted metabasalts will not become negatively buoyant with respect to the mantle until complete melt depletion at 940°C – the upper temperature limit of a steady-state hot zone. Mafic restites are therefore density-stable to higher temperatures in arcs with thinner crust. If arc roots at 1.5 GPa do not experience temperatures sufficient for melt depletion of basaltic restite, the residue may not founder. Thus, whereas the cumulate root sinks at this pressure, the restitic portion of the root may remain positively buoyant until an influx of heat or fluids catalyzes further melting and densification. Assuming instantaneous removal of density-unstable rocks, this would lead to a stable lower crust that is on average denser in thinner arcs (~50 km) compared to thicker arcs (~65 km).

To test our hypothesis, we envision a 50-km-thick arc with mafic lower crust. Slow rates of basalt injection into the hot zone and/or a large distance between mafic rock and the heat source may result in a temperature range high enough to induce melting (>800°C) but low enough to prevent melt depletion (<940°C). The mafic, melt-bearing restite in this scenario achieves densities between 3.15 and 3.3 g/cm^3 and is preserved in the hot zone. Based on seismic velocity and heat-flow constraints, Hacker *et al*. (2015) estimate the density of average lower crust to be between 2.9-3.2 g/cm^3. Due to isostasy, the presence of even denser mafic restites in the lower crust will decrease the elevation of the arc region relative to average continental crust. How does the preservation of a very dense, yet gravitationally stable restitic root affect the elevation of the arc? Assuming Airy isostatic equilibrium, we calculate the relative elevation (H) of an arc with 50-km-thick crust using the equation

$$H = \frac{h_a\rho_a + h_x\rho_x - h_c\rho_c + \rho_m(h_c - h_x - h_a)}{\rho_m} \quad (2)$$

where the subscripts *a, c, x,* and *m* represent the average continental crust, the upper crust of the arc, the residual root of the arc, and the underlying mantle, respectively, while h is the thickness

and ρ is the density of each layer. According to Equation 2 and Figure 9a, and following the crustal structure of Paleozoic to Mesozoic orogens (Hacker *et al*., 2015), we first calculate the elevation of the arc assuming 3 g/cm^3-dense lower crust makes up one-fourth (12.5 km) of the continental crust. In this case, the relative elevation of the arc is ~2.4 km (Fig. 9b), in good agreement with the mean elevation of 50-km-thick crust (Fig. 10). Increasing the density of the lower crust to 3.1-3.3 g/cm^3 accounts for the preservation of mafic restitic material and reduces the elevation of the arc by 400-1100 m (Fig. 9b). If further melting and depletion occur, restites achieve densities sufficient to sink, resulting in isostatic and dynamic uplift of the overlying arc. These processes may therefore contribute to the huge span of elevations (0-5 km relative to sea level) observed for 50-55 km-thick crust (Fig. 10).

In comparison, in both thick and thin arcs, partial melting of metasedimentary crust generates gravitationally stable, alkali feldspar + garnet + quartz-bearing residues with densities between 2.9-3.25 g/cm^3 (Fig. 5). These residues are not arclogites, consistent with the fact that arclogites do not have sediment-like δ^{18}O values. Instead, these metasedimentary restites remain in the lower crust (Fig. 4b), contributing to the thickness, geochemistry, and seismic structure of the bulk arc. Indeed, Hacker *et al*. (2015) argue that heat production and seismic wavespeed data for average lower crust can be satisfied by a felsic composition (up to 66 wt.% SiO_2); this is in good agreement with the compositions of metapelite and metagraywacke restites produced by our models (Supplementary Table S1).

Mass transfer and melting during root removal

Residues can founder with up to 10 vol.% entrained melt, a portion of which may be transported into the mantle within the sinking root. The amount of melt that can be carried to depth versus the

percentage that escapes the residue relies in part on the existence of permeability pathways and pressure gradients large enough to squeeze the melt out of the system (Elkins-Tanton, 2007). Faster roots are also able to transport greater volumes of melt to depth. Importantly, fluids with high viscosities (such as felsic melts) or those entrained within arclogites with low porosities (possible at the confining pressures of upper mantle depths) are more likely to be retained by the descending drip. Therefore, because some percentage of hydrous, incompatible element-rich intermediate melt is probably carried into the upper mantle by the downgoing arclogite, root removal may promote metasomatic alteration and refertilization of the mantle wedge. Furthermore, melts trapped within descending arclogitic masses may have isotopic signatures indicating previous assimilation of the overlying continental crust. These melts, along with the arclogite, may form a volumetrically minor yet isotopically distinct mantle reservoir resembling recycled continental crust (Tatsumi, 2000; Ducea *et al*., 2021b), especially since 25-60% mafic residues are estimated to have foundered over geologic time (Plank, 2005).

In addition, negatively buoyant restites and cumulates, specifically those formed at 1.5 GPa, can contain abundant amphibole. Removal of the amphibole-bearing subarc root transfers water back into the mantle (Davidson *et al*., 2007) and can induce melting of the surrounding asthenosphere (Elkins-Tanton, 2007). More significantly, the presence of amphibole can lead to dehydration melting of the arc root as it descends to higher pressures and temperatures. "Syn-drip" pyroxenite-derived melts, or components thereof, have been documented in the central Andes (Ducea *et al*., 2013; Murray *et al*., 2015; Blum-Oeste & Wörner, 2016), Sierra Nevada (Farmer *et al*., 2002), and northern Iran (Rostami-Hossouri *et al*., 2020). Such melts are alkali-rich, nepheline-normative, and silica-poor (Hirschmann *et al*., 2003; Lambart *et al*., 2013; Ducea *et al*., 2021b). Because arclogites are putative reservoirs of copper sulfides (Chen *et al*., 2020), melting of the foundering arclogite may produce copper-rich magma such that root removal and

porphyry copper deposit genesis may be intimately linked. However, although root-derived melts are becoming increasingly recognized in orogenic systems, the role of arclogite partial melting in contributing to arc magmatism and ore deposit formation has yet to be constrained.

Implications for the Cordilleran cycle model

The Cordilleran cycle model relies on the melting of fertile crust and/or mantle lithosphere underthrust into the subarc hot zone to fuel high-flux magmatic events (DeCelles *et al*., 2009). Production and subsequent removal of dense residues during high-flux events permits further underthrusting and renewal of the cycle. For an arc root comprised of refractory garnet ± amphibole-bearing pyroxenite – a likely scenario if the root is mostly composed of arclogitic cumulates – root removal beneath the active arc will not occur until melt volumes drop below ~10-18%, after which melt substantially accelerates removal. If trapped melt is present in the melt-depleted root, then the periodicity of the Cordilleran cycle may reflect the thermal regime of the subarc lower crust: hotter geotherms will sustain higher average melt fractions, leading to longer periods between high-flux events, while the opposite is true for colder arcs with lower melt fractions. In contrast, the relationship between thermal regime and root removal is reversed if arclogites are primarily restitic, especially at 1.5 GPa. The susceptibility of a restitic root to foundering is heavily dependent on the degree of melt depletion, requiring high temperatures to drive densification and removal of basalt-derived restites. In this case, hotter geotherms promote shorter Cordilleran cycles. There are thus a number of variables (e.g. thermal regime, presence of melt, cumulate *vs*. restitic arclogite) controlling the susceptibility and rate of root removal, which may explain why the duration of lulls in Cordilleran magmatism is so variable, lasting anywhere between 5 and 70 Myr (Chapman *et al*., 2021).

Our conclusions above do not consider metasedimentary residues of partial melting. In arcs with 50-65 km-thick crust, metasedimentary restites are alkali feldspar-rich rocks that are gravitationally stable in the lower crust. Similar density-stable assemblages can be generated by partial melting of tonalite at 1.5 and 2 GPa (Patiño Douce & McCarthy, 1998; Patiño Douce, 2005). In Cordilleran systems, compressional shortening (DeCelles *et al*., 2009) and/or landward arc migration (Chapman & Ducea, 2019) buries foreland lithosphere beneath the arc. If this lithosphere is felsic to intermediate in composition, enhanced melting will ensue, but the accompanying residues will not founder, thus clogging the mantle wedge with melt-depleted restites. Such a process hinders further melting and advancement of the cycle. In contrast, the transport of mafic foreland lithosphere to the hot zone allows the Cordilleran cycle to proceed as envisioned by DeCelles *et al*. (2009). Thus, the tectonomagmatic processes that occur during the Cordilleran cycle depend on the nature of assimilated lower crust.

Alternative models to the Cordilleran cycle have been proposed by a number of researchers, who report evidence for only a secondary role of fusible continental lithosphere in generating high-flux events (Kirsch *et al*., 2016; Decker *et al*., 2017; Schwartz *et al*., 2017; Martínez Ardila *et al*., 2019; Attia *et al*., 2020; Klein *et al*., 2020; Yang *et al*., 2020). These workers argue for more minor (10-40%) crustal assimilation and instead point to external controls on the cyclicity of arc magmatism. In these models, flare-up events are triggered by particularly high fluxes of mantle-derived basalts into the subarc hot zone. This could be caused by (1) higher convergence rates (e.g. Hughes & Mahood, 2008; Zellmer, 2008), which promote hydration and melting of the mantle wedge (Cagnioncle *et al*., 2007), (2) efficient melt focusing within the mantle wedge (Klein *et al*., 2020), or (3) temporary storage of asthenosphere-derived basalt in the mantle lithosphere followed by high-flux melting (Chapman *et al*., 2021). Our results are broadly consistent with cyclic magmatism driven by any of these external processes.

In summary, we investigate the formation and foundering ability of the residual subarc root during magma flare-ups. Results presented in this paper provide insight into the relationships between high-flux magmatism, arclogite foundering, and delivery of fertile lithosphere to the subarc region, but significant uncertainties abound. For example, the nature of the lower crust of the Cordilleran arc and hinterland region is generally unknown. In addition, the importance of relamination of subducted sediments to the base of the arc is still largely unconstrained. Because relamination as well as underthrusting and underplating of melt-fertile lithologies drives crustal anatexis and restite production, additional studies investigating open-system partial melting of a variety of crustal lithologies are required to fully constrain whether the mineralogies and densities of the restites are conducive to foundering. If not, melting of evolved lithologies transferred to the hot zone will result in significant crustal thickening as buoyant residues accumulate in the subarc region.

CONCLUSIONS

We present in this paper calculations and phase equilibria models detailing the effects of crystallization, partial melting, and the presence of entrained melt on the density, viscosity, mineralogy, and overall foundering ability of the arc root. Four main results, summarized below, emerge from these models:

1) One way to offset the negative buoyancy of Cordilleran subarc roots and to retain the root in the lower crust is to add ≥10-18 vol.% hydrous intermediate melt. The presence of melt volumes less than 10-18%, on the other hand, promotes rapid removal of the dense subarc root by significantly reducing the viscosity of the arclogitic mass. In fact, we estimate that the addition of just 5 vol.% melt decreases the time for foundering by around an order of magnitude.

2) Within the deep crustal hot zone of an active arc, isobaric batch crystallization of basaltic magma at 1.5 and 2 GPa generates garnet pyroxenitic cumulates that are gravitationally unstable until near-complete (>80%) crystallization is achieved. Melt extraction prior to 80% crystallization leaves behind cumulates composed of garnet, clinopyroxene, and at 1.5 GPa, amphibole. With densities >3.35 g/cm^3, these cumulates will sink into the underlying mantle.

3) High-pressure partial melting of amphibolitic lower crust and solidified basaltic underplates in the hot zone coupled with incremental melt loss at the MCT generates melt-depleted, density-unstable arclogitic restites.

4) Open-system partial melting of metasedimentary lithologies in the hot zone does not form arclogitic assemblages capable of foundering. Instead, this process results in low-density garnet + alkali feldspar + quartz ± kyanite/sillimanite ± clinopyroxene-bearing restites that remain gravitationally stable in the lower crust at all modeled pressures and temperatures.

Results presented in this paper have broad implications for the processes that occur during the Cordilleran cycle, summarized below:

1) At thinner arcs (~50 km), higher temperatures (>940^{o}C) are required to produce melt-depleted, density-unstable restites from basaltic protoliths. In colder regions of the hot zone, melt depletion of basalt-derived restites may not be achieved, resulting in restites with densities between 3.1-3.3 g/cm^3. These residues are preserved in the lower crust and, due to their high densities, can significantly lower the elevation of the arc.

2) Because arclogites have sufficient density to founder with melt volumes up to 10%, a portion of this melt may be retained to depth within the sinking residue. The influx of

enriched, felsic melts into the mantle may help promote mantle metasomatism and refertilization.

3) The breakdown of "left-over" amphibole in the descending arclogitic root can trigger melting of the surrounding asthenosphere as well as the root itself.

4) Our results as well as published partial melting experiments show that melting of underthrust lithosphere during the Cordilleran cycle likely cannot form a dense root capable of foundering if the underthrust material is felsic to intermediate in composition, thus clogging the mantle wedge and disrupting the cycle according to the Cordilleran cycle model of DeCelles *et al*. (2009). Models invoking external forces to drive high-flux magmatism may thus be more robust in describing the mechanisms behind Cordilleran cyclicity.

ACKNOWLEDGEMENTS

M.N.D. acknowledges support from U.S. NSF grants EAR1725002 and EAR2020935 and the Romanian Executive Agency for Higher Education, Research, Development, and Innovative Funding (UEFISCDI) project PN-III-P4-ID-PCCF-2016-0014. A.T. acknowledges support from the Université Claude Bernard de Lyon with the "BQR Accueil EC 2021" as well as from the F.R.S.-FNRS for the PROBARC project (Grant CR n°1. B. 414.20F). We thank Editor Gerhard Wörner for the constructive comments and efficient handling of the manuscript. Insightful reviews by Michael Farner and an anonymous reviewer greatly improved the manuscript.

REFERENCES

Abers, G. A. & Hacker, B. R. (2016). A MATLAB toolbox and Excel workbook for calculating the densities, seismic wave speeds, and major element composition of minerals and rocks at pressure and temperature. *Geochemistry, Geophysics, Geosystems* **17**, 616-624.

Ague, J. J. (1991). Evidence for major mass transfer and volume strain during regional metamorphism of pelites. *Geology* **19**, 855–858.

Allmendinger, R. W., Jordan, T. E., Kay, S. M. & Isacks, B. L. (1997). The evolution of the Altiplano-Puna plateau of the Central Andes. *Annual Review of Earth and Planetary Sciences* **25**, 139–174.

Annen, C. & Sparks, R. S. J. (2002). Effects of repetitive emplacement of basaltic intrusions on thermal evolution and melt generation in the crust. *Earth and Planetary Science Letters* **203**, 937–955.

Annen, C., Blundy, J. D. & Sparks, R. S. J. (2006). The genesis of intermediate and silicic magmas in deep crustal hot zones. *Journal of Petrology* **47**, 505–539.

Annen, C., Blundy, J. D., Leuthold, J. & Sparks, R. S. J. (2015). Construction and evolution of igneous bodies: Towards an integrated perspective of crustal magmatism. *Lithos* **230**, 206–221.

Attia, S., Cottle, J. M. & Paterson, S. R. (2020). Erupted zircon record of continental crust formation during mantle driven arc flare-ups. *Geology* **48**, 446–451.

Auzanneau, E., Vielzeuf, D. & Schmidt, M. W. (2006). Experimental evidence of decompression melting during exhumation of subducted continental crust. *Contributions to Mineralogy and Petrology* **152**, 125–148.

Beck, S. L. & Zandt, G. (2002). The nature of orogenic crust in the central Andes. *Journal of Geophysical Research: Solid Earth* **107**, 2230.

Beck, S. L., Zandt, G., Myers, S. C., Wallace, T. C., Silver, P. G. & Drake, L. (1996). Crustal-thickness variations in the central Andes. *Geology* **24**, 407–410.

Behn, M. D., Hirth, G. & Kelemen, P. B. (2007). Trench-Parallel Anisotropy Produced by Foundering of Arc Lower Crust. *Science* **317**, 108–111.

Bird, P. (1979). Continental Delamination and the Colorado Plateau. *Journal of Geophysical Research* **84**, 7561–7571.

Bloch, E., Ibañez-Mejia, M., Murray, K., Vervoort, J. & Müntener, O. (2017). Recent crustal foundering in the Northern Volcanic Zone of the Andean arc: Petrological insights from the roots of a modern subduction zone. *Earth and Planetary Science Letters* **476**, 47–58.

Blum-Oeste, M. & Wörner, G. (2016). Central Andean magmatism can be constrained by three ubiquitous end-members. *Terra Nova* **28**, 434–440.

Bons, P. D., Arnold, J., Elburg, M. A., Kalda, J., Soesoo, A. & van Milligen, B. P. (2004). Melt extraction and accumulation from partially molten rocks. *Lithos* **78**, 25–42.

Bottinga, Y. & Weill, D. F. (1970). Densities of liquid silicate systems calculated from partial molar volumes of oxide components. *American Journal of Science* **269**, 169–182.

Brasse, H., Lezaeta, P., Rath, V., Schwalenberg, K., Soyer, W. & Haak, V. (2002). The Bolivian Altiplano conductivity anomaly. *Journal of Geophysical Research* **107**, 2096.

Brown, M. (1994). The generation, segregation, ascent and emplacement of granite magma: the migmatite-to-crustally-derived granite connection in thickened orogens. *Earth-Science Reviews* **36**, 83–130.

Brown, M. (2004). The mechanism of melt extraction from lower continental crust of orogens. *Earth and Environmental Science Transactions of the Royal Society of Edinburgh* **95**, 35–48.

Brown, M. (2007). Crustal melting and melt extraction, ascent and emplacement in orogens: Mechanisms and consequences. *Journal of the Geological Society* **164**, 709–730.

Brown, M. (2010). Melting of the continental crust during orogenesis: the thermal, rheological, and compositional consequences of melt transport from lower to upper continental crust. *Canadian Journal of Earth Sciences* **47**, 655–694.

Bucholz, C. E., Jagoutz, O., Schmidt, M. W. & Sambuu, O. (2014). Fractional crystallization of high-K arc magmas: biotite- versus amphibole-dominated fractionation series in the Dariv Igneous Complex, Western Mongolia. *Contributions to Mineralogy and Petrology* **168**, 1–28.

Cagnioncle, A. M., Parmentier, E. M. & Elkins-Tanton, L. T. (2007). Effect of solid flow above a subducting slab on water distribution and melting at convergent plate boundaries. *Journal of Geophysical Research: Solid Earth* **112**, 1–19.

Cashman, K. V., Sparks, R. S. J. & Blundy, J. D. (2017). Vertically extensive and unstable magmatic systems: A unified view of igneous processes. *Science* **355**, eaag3055.

Chapman, J. B. & Ducea, M. N. (2019). The role of arc migration in Cordilleran orogenic cyclicity. *Geology* **47**, 627–631.

Chapman, J. B., Ducea, M. N., DeCelles, P. G. & Profeta, L. (2015). Tracking changes in crustal thickness during orogenic evolution with Sr/Y: An example from the North American Cordillera. *Geology* **43**, 919–922.

Chapman, J. B., Greig, R. & Haxel, G. B. (2019). Geochemical evidence for an orogenic plateau in the southern U.S. and northern Mexican Cordillera during the Laramide orogeny. *Geology* **48**, 164–168.

Chapman, J. B., Shields, J. E., Ducea, M. N., Paterson, S. R., Attia, S. & Ardill, K. E. (2021). The causes of continental arc flare ups and drivers of episodic magmatic activity in Cordilleran orogenic systems. *Lithos* **398–399**, 106307.

Chen, K., Tang, M., Lee, C. T. A., Wang, Z., Zou, Z., Hu, Z. & Liu, Y. (2020). Sulfide-bearing cumulates in deep continental arcs: The missing copper reservoir. *Earth and Planetary Science Letters* **531**, 115971.

Chin, E. J., Lee, C. T. A., Tollstrup, D. L., Xie, L., Wimpenny, J. B. & Yin, Q. Z. (2013). On the origin of hot metasedimentary quartzites in the lower crust of continental arcs. *Earth and Planetary Science Letters* **361**, 120–133.

Clemens, J. D. & Stevens, G. (2016). Melt segregation and magma interactions during crustal melting: Breaking out of the matrix. *Earth-Science Reviews* **160**, 333–349.

Clemens, J. D. & Vielzeuf, D. (1987). Constraints on melting and magma production in the crust. *Earth and Planetary Science Letters* **86**, 287–306.

Collins, W. J., Huang, H. Q. & Jiang, X. (2016). Water-fluxed crustal melting produces Cordilleran batholiths. *Geology* **44**, 143–146.

Collins, W. J., Murphy, J. B., Johnson, T. E. & Huang, H. Q. (2020). Critical role of water in the formation of continental crust. *Nature Geoscience* **13**, 331–338.

Comeau, M. J., Unsworth, M. J. & Cordell, D. (2016). New constraints on the magma distribution and composition beneath Volcán Uturuncu and the southern Bolivian Altiplano from magnetotelluric data. *Geosphere* **12**, 1391–1421.

Comeau, M. J., Unsworth, M. J., Ticona, F. & Sunagua, M. (2015). Magnetotelluric images of magma distribution beneath Volcán Uturuncu, Bolivia: Implications for magma dynamics. *Geology* **43**, 243–246.

Connolly, J. A. D. (2009). The geodynamic equation of state: What and how. *Geochemistry, Geophysics, Geosystems* **10**, Q10014.

Connolly, J. A. D. (2005). Computation of phase equilibria by linear programming: A tool for geodynamic modeling and its application to subduction zone decarbonation. *Earth and Planetary Science Letters* **236**, 524–541.

Conrad, C. P. (2000). Convective instability of thickening mantle lithosphere. *Geophysical Journal International* **143**, 52–70.

Currie, C. A., Ducea, M. N., DeCelles, P. G. & Beaumont, C. (2015). Geodynamic models of Cordilleran orogens: Gravitational instability of magmatic arc roots. In: DeCelles, P. G., Ducea, M. N., Carrapa, B. & Kapp, P. A. (ed.) *Geodynamics of a Cordilleran Orogenic System: The Central Andes of Argentina and North Chile*. The Geological Society of America **212**, 1–22.

Daczko, N. R., Piazolo, S., Meek, U., Stuart, C. A. & Elliott, V. (2016). Hornblendite delineates zones of mass transfer through the lower crust. *Scientific Reports* **6**, 1-6.

Davidson, J., Turner, S., Handley, H., Macpherson, C. & Dosseto, A. (2007). Amphibole "sponge" in arc crust? *Geology* **35**, 787–790.

Davies, J. H. & Stevenson, D. J. (1992). Physical model of source region of subduction zone volcanics. *Journal of Geophysical Research* **97**, 2037–2070.

DeCelles, P. G., Ducea, M. N., Kapp, P. & Zandt, G. (2009). Cyclicity in Cordilleran orogenic systems. *Nature Geoscience* **2**, 251–257.

DeCelles, P. G. *et al.* (2015a). Cyclical orogenic processes in the Cenozoic central Andes. In: DeCelles, P. G., Ducea, M. N., Carrapa, B. & Kapp, P. A. (ed.) *Geodynamics of a Cordilleran Orogenic System: The Central Andes of Argentina and North Chile*. The Geological Society of America **212**, 459–490.

DeCelles, P. G. *et al.* (2015b). The Miocene Arizaro Basin, central Andean hinterland: Response to partial lithosphere removal? In: DeCelles, P. G., Ducea, M. N., Carrapa, B. & Kapp, P. A. (ed.) *Geodynamics of a Cordilleran Orogenic System: The Central Andes of Argentina and North Chile*. The Geological Society of America **212**, 359-386.

Decker, M., Schwartz, J. J., Stowell, H. H., Klepeis, K. A., Tulloch, A. J., Kitajima, K., Valley, J. W. & Kylander-Clark, A. R. C. (2017). Slab-Triggered Arc Flare-up in the cretaceous median batholith and the growth of lower arc crust, Fiordland, New Zealand. *Journal of Petrology* **58**, 1145–1171.

Delph, J. R., Ward, K. M., Zandt, G., Ducea, M. N. & Beck, S. L. (2017). Imaging a magma plumbing system from MASH zone to magma reservoir. *Earth and Planetary Science Letters* **457**, 313–324.

DePaolo, D. J. (1981). Trace element and isotopic effects of combined wallrock assimilation and fractional crystallization. *Earth and Planetary Science Letters* **53**, 189–202.

Depine, G. V., Andronicos, C. L. & Phipps-Morgan, J. (2008). Near-isothermal conditions in the middle and lower crust induced by melt migration. *Nature* **452**, 80–83.

Dhuime, B., Bosch, D., Garrido, C. J., Bodinier, J. L., Bruguier, O., Hussain, S. S. & Dawood, H. (2009). Geochemical architecture of the lower- to middle-crustal section of a Paleo-island arc (Kohistan Complex, Jijal-Kamila area, Northern Pakistan): Implications for the evolution of an oceanic subduction zone. *Journal of Petrology* **50**, 531–569.

Diener, J. F. A. & Fagereng, Å. (2014). The influence of melting and melt drainage on crustal rheology during orogenesis. *Journal of Geophysical Research: Solid Earth* **119**, 6193–6210.

Dodge, F. C. W., Lockwood, J. P. & Calk, L. C. (1988). Fragments of the mantle and crust from beneath the Sierra Nevada batholith: Xenoliths in a volcanic pipe near Big Creek, California. *Geological Society of America Bulletin* **100**, 938-947.

Ducea, M. N., Seclaman, A. C., Murray, K. E., Jianu, D. & Schoenbohm, L. M. (2013). Mantle-drip magmatism beneath the Altiplano-Puna plateau, central Andes. *Geology* **41**, 915–918.

Ducea, M. N. (2002). Constraints on the bulk composition and root foundering rates of continental arcs: A California arc perspective. *Journal of Geophysical Research: Solid Earth* **107**, 2304.

Ducea, M. N. & Barton, M. D. (2007). Igniting flare-up events in Cordilleran arcs. *Geology* **35**, 1047–1050.

Ducea, M. N. & Chapman, A. D. (2018). Sub-magmatic arc underplating by trench and forearc materials in shallow subduction systems; A geologic perspective and implications. *Earth-Science Reviews* **185**, 763–779.

Ducea, M. N., Chapman, A. D., Bowman, E. & Balica, C. (2021b). Arclogites and their role in continental evolution; part 2: Relationship to batholiths and volcanoes, density and foundering, remelting and long-term storage in the mantle. *Earth-Science Reviews* **214**, 103476.

Ducea, M. N., Chapman, A. D., Bowman, E. & Triantafyllou, A. (2021a). Arclogites and their role in continental evolution; part 1: Background, locations, petrography, geochemistry, chronology and thermobarometry. *Earth-Science Reviews* **214**, 103375.

Ducea, M. N., Saleeby, J. B. & Bergantz, G. (2015). The architecture, chemistry, and evolution of continental magmatic arcs. *Annual Review of Earth and Planetary Sciences* **43**, 299–331.

Ducea, M. N. & Saleeby, J. B. (1996). Buoyancy sources for a large, unrooted mountain range, the Sierra Nevada, California: Evidence from xenolith thermobarometry. *Journal of Geophysical Research* **101**, 8229–8244.

Ducea, M. & Saleeby, J. (1998). A case for delamination of the deep batholithic crust beneath the Sierra Nevada, California. *International Geology Review* **40**, 78–93.

Dufek, J. & Bergantz, G. W. (2005). Lower crustal magma genesis and preservation: A stochastic framework for the evaluation of basalt-crust interaction. *Journal of Petrology* **46**, 2167–2195.

Elkins-Tanton, L. T. (2007). Continental magmatism, volatile recycling, and a heterogeneous mantle caused by lithospheric gravitational instabilities. *Journal of Geophysical Research: Solid Earth* **112**, 1–13.

Erdman, M. E., Lee, C. T. A., Levander, A. & Jiang, H. (2016). Role of arc magmatism and lower crustal foundering in controlling elevation history of the Nevadaplano and Colorado Plateau: A case study of pyroxenitic lower crust from central Arizona, USA. *Earth and Planetary Science Letters* **439**, 48–57.

Esperança, S., Carlson, R. W. & Shirey, S. B. (1988). Lower crustal evolution under central Arizona: Sr, Nd and Pb isotopic and geochemical evidence from the mafic xenoliths of Camp Creek. *Earth and Planetary Science Letters* **90**, 26–40.

Farmer, G. L., Glazner, A. F. & Manley, C. R. (2002). Did lithospheric delamination trigger late Cenozoic potassic volcanism in the southern Sierra Nevada, California? *Bulletin of the Geological Society of America* **114**, 754–768.

Ferrari, L., Orozco-Esquivel, T., Manea, V. & Manea, M. (2012). The dynamic history of the Trans-Mexican Volcanic Belt and the Mexico subduction zone. *Tectonophysics* **522–523**, 122–149.

Garzione, C. N. *et al.* (2008). Rise of the Andes. *Science* **320**, 1304–1307.

Garzione, C. N., Molnar, P., Libarkin, J. C. & MacFadden, B. J. (2006). Rapid late Miocene rise of the Bolivian Altiplano: Evidence for removal of mantle lithosphere. *Earth and Planetary Science Letters* **241**, 543–556.

Gehrels, G. et al. (2009). U-Th-Pb geochronology of the Coast Mountains batholith in north-coastal British Columbia: Constraints on age and tectonic evolution. *GSA Bulletin* **121**, 1341–1361.

Ghosh, P., Garzione, C. N., Eiler, J. M. (2006). Rapid uplift of the Altiplano revealed through ^{13}C-^{18}O bonds in paleosol carbonates. *Science* **311**, 511-515.

Göğüş, O. H. & Pysklywec, R. N. (2008). Near-surface diagnostics of dripping or delaminating lithosphere. *Journal of Geophysical Research: Solid Earth* **113**, 1–11.

Green, A. R., DeBari, S. M., Kelemen, P. B., Blusztajn, J. & Clift, P. D. (2006). A detailed geochemical study of island Arc crust: The Talkeetna Arc section, south-central Alaska. *Journal of Petrology* **47**, 1051–1093.

Green, D. H., Hibberson, W. O., Rosenthal, A., Kovács, I., Yaxley, G. M., Falloon, T. J. & Brink, F. (2014). Experimental Study of the Influence of Water on Melting and Phase Assemblages in the Upper Mantle. *Journal of Petrology* **55**, 2067–2096.

Green, E. C. R., White, R. W., Diener, J. F. A., Powell, R., Holland, T. J. B. & Palin, R. M. (2016). Activity–composition relations for the calculation of partial melting equilibria in metabasic rocks. *Journal of Metamorphic Geology* **34**, 845–869.

Grove, T. L., Till, C. B. & Krawczynski, M. J. (2012). The role of H 2O in subduction zone magmatism. *Annual Review of Earth and Planetary Sciences* **40**, 413–439.

Guernina, S. & Sawyer, E. W. (2003). Large-scale melt-depletion in granulite terranes: An example from the Archean Ashuanipi subprovince of Quebec. *Journal of Metamorphic Geology* **21**, 181–201.

Gysi, A. P., Jagoutz, O., Schmidt, M. & Targuisti, K. (2011). Petrogenesis of pyroxenites and melt infiltrations in the ultramafic complex of Beni Bousera, northern Morocco. *Journal of Petrology* **52**, 1679–1735.

Hacker, B. R., Kelemen, P. B. & Behn, M. D. (2011). Differentiation of the continental crust by relamination. *Earth and Planetary Science Letters* **307**, 501–516.

Hacker, B. R., Kelemen, P. B. & Behn, M. D. (2015). Continental lower crust. *Annual Review of Earth and Planetary Sciences* **43**, 167–205.

Hacker, B. R., Mehl, L., Kelemen, P. B., Rioux, M., Behn, M. D. & Luffi, P. (2008). Reconstruction of the Talkeetna intraoceanic arc of Alaska through thermobarometry. *Journal of Geophysical Research: Solid Earth* **113**, 1–16.

Hacker, B. *et al.* (2005). Near-ultrahigh pressure processing of continental crust: Miocene crustal xenoliths from the Pamir. *Journal of Petrology* **46**, 1661–1687.

Handy, M. R., Mulch, A., Rosenau, M. & Rosenberg, C. L. (2001). The role of fault zones and melts as agents of weakening, hardening and differentiation of the continental crust: a synthesis. *Geological Society, London, Special Publications* **186**, 305-332.

Haschke, M. R., Scheuber, E., Günther, A. & Reutter, K. J. (2002). Evolutionary cycles during the Andean orogeny: Repeated slab breakoff and flat subduction? *Terra Nova* **14**, 49–55.

Hildreth, W. & Moorbath, S. (1988). Crustal contributions to arc magmatism in the Andes of Central Chile. *Contributions to Mineralogy and Petrology* **98**, 455–489.

Hirschmann, M. M., Kogiso, T., Baker, M. B. & Stolper, E. M. (2003). Alkalic magmas generated by partial melting of garnet pyroxenite. *Geology* **31**, 481–484.

Holland, T. J. B. & Powell, R. (2011). An improved and extended internally consistent thermodynamic dataset for phases of petrological interest, involving a new equation of state for solids. *Journal of Metamorphic Geology* **29**, 333–383.

Holness, M. B. (2006). Melt–Solid Dihedral Angles of Common Minerals in Natural Rocks. *Journal of Petrology* **47**, 791–800.

Holness, M. B. & Sawyer, E. W. (2008). On the Pseudomorphing of Melt-filled Pores During the Crystallization of Migmatites. *Journal of Petrology* **49**, 1343–1363.

Hoorn, C. *et al.* (2010). Amazonia Through Time: Andean Amazonia through time: Andean uplift, climate change, landscape evolution, and biodiversity. *Science* **330**, 927–931.

Houseman, G. A., McKenzie, D. P. & Molnar, P. (1981). Convective instability of a thickened boundary layer and its relevance for the thermal evolution of continental convergent belts. *Journal of Geophysical Research* **86**, 6115–6132.

Huang, H., Lin, F., Schmandt, B., Farrell, J., Smith, R. B. & Tsai, V. C. (2015). The Yellowstone magmatic system from the mantle plume to the upper crust. *Science* **348**, 773–776.

Hughes, G. R. & Mahood, G. A. (2008). Tectonic controls on the nature of large silicic calderas in volcanic arcs. *Geology* **36**, 627–630.

Jackson, M. D., Blundy, J., & Sparks, R. S. J. (2018). Chemical differentiation, cold storage and remobilization of magma in the Earth's crust. *Nature* **564**, 405-409.

Jagoutz, O. & Schmidt, M. W. (2012). The formation and bulk composition of modern juvenile continental crust: The Kohistan arc. *Chemical Geology* **298**–**299**, 79–96.

Jagoutz, O. & Schmidt, M. W. (2013). The composition of the foundered complement to the continental crust and a re-evaluation of fluxes in arcs. *Earth and Planetary Science Letters* **371**–**372**, 177–190.

Jagoutz, O. E., Burg, J. P., Hussain, S., Dawood, H., Pettke, T., Iizuka, T. & Maruyama, S. (2009). Construction of the granitoid crust of an island arc part I: Geochronological and geochemical constraints from the plutonic Kohistan (NW Pakistan). *Contributions to Mineralogy and Petrology* **158**, 739–755.

Jagoutz, O. & Kelemen, P. B. (2015). Role of arc processes in the formation of continental crust. *Annual Review of Earth and Planetary Sciences* **43**, 363–404.

Jagoutz, O. & Klein, B. (2018). On the importance of crystallization-differentiation for the generation of SiO2-rich melts and the compositional build-up of ARC (and continental) crust. *American Journal of Science* **318**, 29–63.

Jin, Z. M., Zhang, J., Green, I. W. & Jin, S. (2001). Eclogite rheology: Implication for subducted lithosphere. *Geology* **29**, 667–670.

Jones, C. H., Farmer, G. L. & Unruh, J. (2004). Tectonics of Pliocene removal of lithosphere of the Sierra Nevada, California. *GSA Bulletin* **116**, 1408-1422.

Jull, M. & Kelemen, P. B. (2001). On the conditions for lower crustal convective instability. *Journal of Geophysical Research: Solid Earth* **106**, 6423–6446.

Kay, R. W. & Mahlburg Kay, S. (1993). Delamination and delamination magmatism. *Tectonophysics* **219**, 177–189.

Kay, S. M., Coira, B. & Viramonte, J. (1994). Young mafic back arc volcanic rocks as indicators of continental lithospheric delamination beneath the Argentine Puna plateau, central Andes. *Journal of Geophysical Research* **99**, 24323–24339.

Keller, C. B., Schoene, B., Barboni, M., Samperton, K. M. & Husson, J. M. (2015). Volcanic-plutonic parity and the differentiation of the continental crust. *Nature* **523**, 301–307.

Kelly, R. K., Kelemen, P. B. & Jull, M. (2003). Buoyancy of the continental upper mantle. *Geochemistry, Geophysics, Geosystems* **4**, 1017.

Kidder, S., Ducea, M., Gehrels, G., Patchett, P. J. & Vervoort, J. (2003). Tectonic and magmatic development of the Salinian Coast Ridge Belt, California. *Tectonics* **22**, 1-20.

Kirsch, M., Paterson, S. R., Wobbe, F., Ardila, A. M. M., Clausen, B. L. & Alasino, P. H. (2016). Temporal histories of Cordilleran continental arcs: Testing models for magmatic episodicity. *American Mineralogist* **101**, 2133–2154.

Klein, B. Z., Jagoutz, O. & Ramezani, J. (2021). High-precision geochronology requires that ultrafast mantle-derived magmatic fluxes built the transcrustal Bear Valley Intrusive Suite, Sierra Nevada, California, USA. *Geology* **49**, 106–110.

Klepeis, K., Webb, L., Blatchford, H., Schwartz, J., Jongens, R., Turnbull, R., Stowell, H. (2019). Deep slab collision during Miocene subduction causes uplift along crustal-scale reverse faults in Fiordland, New Zealand. *GSA Today* **29**, 4-10.

Koch, C. D. et al. (2021). Crustal thickness and magma storage beneath the Ecuadorian arc. *Journal of South American Earth Sciences* **110**, 103331.

Korhonen, F. J., Saito, S., Brown, M. & Siddoway, C. S. (2010). Modeling multiple melt loss events in the evolution of an active continental margin. *Lithos* **116**, 230–248.

Kress, V. C. & Carmichael, I. S. (1991). The compressibility of silicate liquids containing Fe_2O_3 and the effect of composition, temperature, oxygen fugacity and pressure on their redox states. *Contributions to Mineralogy and Petrology* **108**, 82-92.

Krystopowicz, N. J. & Currie, C. A. (2013). Crustal eclogitization and lithosphere delamination in orogens. *Earth and Planetary Science Letters* **361**, 195–207.

Lambart, S., Laporte, D. & Schiano, P. (2013). Markers of the pyroxenite contribution in the major-element compositions of oceanic basalts: Review of the experimental constraints. *Lithos* **160**–**161**, 14–36.

Lange, R. A. & Carmichael, I. S. (1987). Densities of Na_2O-K_2O-CaO-MgO-FeO-Fe_2O_3-Al_2O_3-TiO_2-SiO_2 liquids: new measurements and derived partial molar properties. *Geochimica et Cosmochimica Acta* **51**, 2931-2946.

Langmuir, C. H., Klein, E. M. & Plank, T. (1992). Petrology systematics of mid-ocean ridge basalts: constraints on melt generation beneath ocean ridges. In: Morgan, J. P., Blackman,

D. K. & Sinton, J. M. (ed.) *Mantle Flow and Melt Generation at Mid-Ocean Ridges*. Geophysical Monograph, American Geophysical Union **71**, 183-280.

Laporte, D., Rapaille, C. & Provost, A. (1997). Wetting Angles, Equilibrium Melt Geometry, and the Permeability Threshold of Partially Molten Crustal Protoliths. In: Bouchez, J. L., Hutton, D. H. W. & Stephens, W. E. (ed.) *Granite: From Segregation of Melt to Emplacement Fabrics*. Petrology and Structural Geology **8**, 31-54.

Laske, G., Masters, G., Ma, Z. & Pasyanos, M. (2013). Update on CRUST1.0 – a 1-degree global model of Earth's crust. *European Geological Union, Geophysical Research Abstracts* **15**, 2658.

Le Pourhiet, L., Gurnis, M. & Saleeby, J. (2006). Mantle instability beneath the Sierra Nevada Mountains in California and Death Valley extension. *Earth and Planetary Science Letters* **251**, 104–119.

Lee, C. T. A. (2014). Physics and Chemistry of Deep Continental Crust Recycling. *Treatise on Geochemistry: Second Edition*. Elsevier Ltd.

Lee, C. T. A. & Anderson, D. L. (2015). Continental crust formation at arcs, the arclogite "delamination" cycle, and one origin for fertile melting anomalies in the mantle. *Science Bulletin* **60**, 1141–1156.

Lee, C. T. A., Cheng, X. & Horodyskyj, U. (2006). The development and refinement of continental arcs by primary basaltic magmatism, garnet pyroxenite accumulation, basaltic recharge and delamination: Insights from the Sierra Nevada, California. *Contributions to Mineralogy and Petrology* **151**, 222–242.

Luebert, F. & Muller, L. A. H. (2015). Effects of mountain formation and uplift on biological diversity. *Frontiers in Genetics* **6**, 1-2.

Lupulescu, A. & Watson, E. B. (1999). Low melt fraction connectivity of granitic and tonalitic melts in a mafic crustal rock at 800 °C and 1 GPa. *Contributions to Mineralogy and Petrology* **134**, 202–216.

Mandler, B. E. & Grove, T. L. (2016). Controls on the stability and composition of amphibole in the Earth's mantle. *Contributions to Mineralogy and Petrology* **171**, 68.

Manley, C. R., Glazner, A. F. & Farmer, G. L. (2000). Timing of volcanism in the Sierra Nevada of California: Evidence for Pliocene delamination of the batholithic root? *Geology* **28**, 811–814.

Martin, C. R., Jagoutz, O., Upadhyay, R., Royden, L. H., Eddy, M. P., Bailey, E., Nichols, C. I. O. & Weiss, B. P. (2020). Paleocene latitude of the Kohistan-Ladakh arc indicates multistage India-Eurasia collision. *Proceedings of the National Academy of Sciences of the United States of America* **117**, 29487–29494.

Martínez Ardila, A. M., Paterson, S. R., Memeti, V., Parada, M. A. & Molina, P. G. (2019). Mantle driven cretaceous flare-ups in Cordilleran arcs. *Lithos* **326**–**327**, 19–27.

McGlashan, N., Brown, L. & Kay, S. (2008). Crustal thickness in the central Andes from teleseismically recorded depth phase precursors. *Geophysical Journal International* **175**, 1013–1022.

McKenzie, D. (1984). The Generation and Compaction of Partially Molten Rock. *Journal of Petrology* **25**, 713–765.

Meissner, R. & Mooney, W. (1998). Weakness of the lower continental crust: A condition for delamination, uplift, and escape. *Tectonophysics* **296**, 47–60.

Mibe, K., Kawamoto, T., Matsukage, K. N., Fei, Y. & Ono, S. (2011). Slab melting versus slab dehydration in subduction-zone magmatism. *Proceedings of the National Academy of Sciences of the United States of America* **108**, 8177–8182.

Morfin, S., Sawyer, E. W. & Bandyayera, D. (2013). Large volumes of anatectic melt retained in granulite facies migmatites: An injection complex in northern Quebec. *Lithos* **168**–**169**, 200–218.

Müntener, O., Kelemen, P. B. & Grove, T. L. (2001). The role of H2O during crystallization of primitive arc magmas under uppermost mantle conditions and genesis of igneous pyroxenites: An experimental study. *Contributions to Mineralogy and Petrology* **141**, 643–658.

Müntener, O. & Ulmer, P. (2006). Experimentally derived high-pressure cumulates from hydrous arc magmas and consequences for the seismic velocity structure of lower arc crust. *Geophysical Research Letters* **33**, 1–5.

Murphy, M. & Chapman, A. D. (2018). Rooting around beneath an arc: Zircon U-Pb geochronologic and Hf isotopic constraints on the evolution of the base of the Sierra Nevada batholith. *Geological Society of America, Abstracts with Programs* **50**, 6.

Murray, K. E., Ducea, M. N. & Schoenbohm, L. (2015). Foundering-driven lithospheric melting: The source of central Andean mafic lavas on the Puna Plateau (22°S-27°S). In: DeCelles, P. G., Ducea, M. N., Carrapa, B. & Kapp, P. A. (ed.) *Geodynamics of a Cordilleran Orogenic System: The Central Andes of Argentina and North Chile*. The Geological Society of America **212**, 139–166.

Nandedkar, R. H., Ulmer, P. & Müntener, O. (2014). Fractional crystallization of primitive, hydrous arc magmas: An experimental study at 0.7 GPa. *Contributions to Mineralogy and Petrology* **167**, 1–27.

Otamendi, J. E., Ducea, M. N., Tibaldi, A. M., Bergantz, G. W., de la Rosa, J. D. & Vujovich, G. I. (2009). Generation of tonalitic and dioritic magmas by coupled partial melting of gabbroic

and metasedimentary rocks within the deep crust of the Famatinian magmatic arc, Argentina. *Journal of Petrology* **50**, 841-873.

Otamendi, J. E. & Patiño Douce, A. E. (2001). Partial melting of aluminous metagreywackes in the Northern Sierra de Comechingones, Central Argentina. *Journal of Petrology* **42**, 1751–1772.

Palin, R. M., White, R. W., Green, E. C. R., Diener, J. F. A., Powell, R. & Holland, T. J. B. (2016). High-grade metamorphism and partial melting of basic and intermediate rocks. *Journal of Metamorphic Geology* **34**, 871–892.

Paterson, M. S. (2001). A granular flow theory for the deformation of partially molten rock. *Tectonophysics* **335**, 51–61.

Patiño Douce, A. E. (2005). Vapor-absent melting of tonalite at 15-32 kbar. *Journal of Petrology* **46**, 275–290.

Patiño Douce, A. E. & Beard, J. S. (1995). Dehydration-melting of biotite gneiss and quartz amphibolite from 3 to 15 kbar. *Journal of Petrology* **36**, 707–738.

Patiño Douce, A. E. & Harris, N. (1998). Experimental constraints on Himalayan anatexis. *Journal of Petrology* **39**, 689–710.

Patiño Douce, A. E., & McCarthy, T. C. (1998). Melting of crustal rocks during continental collision and subduction. In: Hacker, B. R. & Liou, J. G. (eds) *When Continents Collide: Geodynamics and Geochemistry of Ultrahigh-Pressure Rocks*. Dordrecht: Kluwer Academic, 27-55.

Petford, N. (1995). Segregation of tonalitic-trondhjemitic melts in the continental crust: The mantle connection. *Journal of Geophysical Research: Solid Earth* **100**, 15735–15743.

Plank, T. (2005). Constraints from Thorium/Lanthanum on sediment recycling at subduction zones and the evolution of the continents. *Journal of Petrology* **46**, 921–944.

Poudjom Djomani, Y. H., O'Reilly, S. Y., Griffin, W. L. & Morgan, P. (2001). The density structure of subcontinental lithosphere through time. *Earth and Planetary Science Letters* **184**, 605–621.

Prouteau, G., Scaillet, B., Pichavant, M. & Maury, R. (2001). Evidence for mantle metasomatism by hydrous silicic melts derived from subducted oceanic crust. *Nature* **410**, 197–200.

Pysklywec, R. N. & Cruden, A. R. (2004). Coupled crust-mantle dynamics and intraplate tectonics: Two-dimensional numerical and three-dimensional analogue modeling. *Geochemistry, Geophysics, Geosystems* **5**, Q10003.

Rabinowicz, M. & Vigneresse, J.-L. (2004). Melt segregation under compaction and shear channeling: Application to granitic magma segregation in a continental crust. *Journal of Geophysical Research: Solid Earth* **109**, B04407.

Rapp, R. P. & Watson, E. B. (1995). Dehydration melting of metabasalt at 8-32 kbar: Implications for continental growth and crust-mantle recycling. *Journal of Petrology* **36**, 891–931.

Rapp, R. P., Watson, E. B. & Miller, C. F. (1991). Partial melting of amphibolite/eclogite and the origin of Archean trondhjemites and tonalites. *Precambrian Research* **51**, 1–25.

Ratschbacher, B. C., Paterson, S. R. & Fischer, T. P. (2019). Spatial and Depth-Dependent Variations in Magma Volume Addition and Addition Rates to Continental Arcs: Application to Global CO2 Fluxes since 750 Ma. *Geochemistry, Geophysics, Geosystems* **20**, 2997–3018.

Rautela, O., Chapman, A. D., Shields, J. E., Ducea, M. N., Lee, C. T., Jiang, H. & Saleeby, J. (2020). In search for the missing arc root of the Southern California Batholith: P-T-t evolution of upper mantle xenoliths of the Colorado Plateau Transition Zone. *Earth and Planetary Science Letters* **547**, 116447.

Redler, C., White, R. W. & Johnson, T. E. (2013). Migmatites in the Ivrea Zone (NW Italy): Constraints on partial melting and melt loss in metasedimentary rocks from Val Strona di Omegna. *Lithos* **175**–**176**, 40–53.

Richards, J. P. (2011). Magmatic to hydrothermal metal fluxes in convergent and collided margins. *Ore Geology Reviews* **40**, 1–26.

Ringuette, L., Martignole, J. & Windley, B. F. (1999). Magmatic crystallization, isobaric cooling, and decompression of the garnet-bearing assemblages of the Jijal sequence (Kohistan terrane, western Himalayas). *Geology* **27**, 139–142.

Rosenberg, C. L. & Handy, M. R. (2001). Mechanisms and orientation of melt segregation paths during pure shearing of a partially molten rock analog (norcamphor–benzamide). *Journal of Structural Geology* **23**, 1917–1932.

Rosenberg, C. L. & Handy, M. R. (2005). Experimental deformation of partially melted granite revisited: Implications for the continental crust. *Journal of Metamorphic Geology* **23**, 19–28.

Rosenberg, C. L., Medvedev, S. & Handy, M. R. (2007). Effects of melting on continental deformation and faulting. In: Handy, M., Hirth, G. & Hovius, N. (eds) *Tectonic Faults: Agents of Change on a Dynamic Earth*. MIT Press, 357-402.

Rostami-Hossouri, M. *et al.* (2020). Geochemistry of continental alkali basalts in the Sabzevar region, northern Iran: implications for the role of pyroxenite in magma genesis. *Contributions to Mineralogy and Petrology* **175**, 1–22.

Ryan, J., Beck, S., Zandt, G., Wagner, L., Minaya, E. & Tavera, H. (2016). Central Andean crustal structure from receiver function analysis. *Tectonophysics* **682**, 120–133.

Saleeby, J., Ducea, M. & Clemens-Knott, D. (2003). Production and loss of high-density batholithic root, southern Sierra Nevada, California. *Tectonics* **22**, 1064.

Sawyer, E. W. (1986). The influence of source rock type, chemical weathering and sorting on the geochemistry of clastic sediments from the Quetico Metasedimentary Belt, Superior Province, Canada. *Chemical Geology* **55**, 77–95.

Sawyer, E. W. (1991). Disequilibrium Melting and the Rate of Melt–Residuum Separation During Migmatization of Mafic Rocks from the Grenville Front, Quebec. *Journal of Petrology* **32**, 701–738.

Sawyer, E. W. (1994). Melt segregation in the continental crust. *Geology* **22**, 1019–1022.

Sawyer, E. W. (2001). Melt segregation in the continental crust: distribution and movement of melt in anatectic rocks. *Journal of Metamorphic Geology* **19**, 291–309.

Schilling, F. R. *et al.* (2006). Partial Melting in the Central Andean Crust: a Review of Geophysical, Petrophysical, and Petrologic Evidence. In: Oncken, O., *et al.* (ed.) *The Andes – Active Subduction Orogeny*. Springer-Vertlag Frontiers in Earth Sciences **1**, 459–474.

Schmid, R. & Wood, B. J. (1976). Phase relationships in granulitic metapelites from the Ivrea-Verbano zone (Northern Italy). *Contributions to Mineralogy and Petrology* **54**, 255–279.

Schmidt, M. W. & Jagoutz, O. (2017). The global systematics of primitive arc melts. *Geochemistry, Geophysics, Geosystems* **18**, 2817–2854.

Schoenbohm, L. M. & Carrapa, B. (2015). Miocene–Pliocene shortening, extension, and mafic magmatism support small-scale lithospheric foundering in the central Andes, NW Argentina. In: DeCelles, P. G., Ducea, M. N., Carrapa, B. & Kapp, P. A. (ed.) *Geodynamics of a Cordilleran Orogenic System: The Central Andes of Argentina and North Chile*. The Geological Society of America **212**, 167-180.

Schwartz, J. J., Klepeis, K. A., Sadorski, J. F., Stowell, H. H., Tulloch, A. J. & Coble, M. A. (2017). The tempo of continental arc construction in the Mesozoic Median Batholith, Fiordland, New Zealand. *Lithosphere* **9**, 8343–365.

Sen, C. & Dunn, T. (1994). Dehydration melting of a basaltic composition amphibolite at 1.5 and 2.0 GPa: implications for the origin of adakites. *Contributions to Mineralogy and Petrology* **117**, 394–409.

Sepulchre, P., Sloan, L. C., Snyder, M. & Fiechter, J. (2009). Impacts of andean uplift on the Humboldt current system: A climate model sensitivity study. *Paleoceanography* **24**, 1–11.

Shea, W. T. & Kronenberg, A. K. (1993). Strength and anisotropy of foliated rocks with varied mica contents. *Journal of Structural Geology* **15**, 1097–1121.

Smith, D., Arculus, R. J., Manchester, J. E. & Tyner, G. N. (1994). Garnet-pyroxene-amphibole xenoliths from Chino Valley, Arizona, and implications for continental lithosphere below the Moho. *Journal of Geophysical Research* **99**, 683–696.

Tatsumi, Y. (2000). Continental crust formation by crustal delamination in subduction zones and complementary accumulation of the enriched mantle I component in the mantle. *Geochemistry, Geophysics, Geosystems* **1**, 2000GC000094.

Tassara, A. (2006). Factors controlling the crustal density structure underneath active continental margins with implications for their evolution. *Geochemistry, Geophysics, Geosystems* **7**, Q01001.

Thybo, H. & Artemieva, I. M. (2013). Moho and magmatic underplating in continental lithosphere. *Tectonophysics* **609**, 605-619.

Triantafyllou, A., Berger, J., Baele, J. M., Bruguier, O., Diot, H., Ennih, N., Monnier, C., Plissart, G., Vandycke, S. & Watlet, A. (2018). Intra-oceanic arc growth driven by magmatic and tectonic processes recorded in the Neoproterozoic Bougmane arc complex (Anti-Atlas, Morocco). *Precambrian Research* **304**, 39-63.

Turner, S. J. & Langmuir, C. H. (2015). The global chemical systematics of arc front stratovolcanoes: Evaluating the role of crustal processes. *Earth and Planetary Science Letters* **422**, 182–193.

Valera, J. L., Negredo, A. M. & Jiménez-Munt, I. (2011). Deep and near-surface consequences of root removal by asymmetric continental delamination. *Tectonophysics* **502**, 257–265.

Vielzeuf, D. & Schmidt, M. W. (2001). Melting relations in hydrous systems revisited: Application to metapelites, metagreywackes and metabasalts. *Contributions to Mineralogy and Petrology* **141**, 251–267.

Vielzeuf, D. & Holloway, J. R. (1988). Experimental determination of the fluid-absent melting relations in the pelitic system. *Contributions to Mineralogy and Petrology* **98**, 257–276.

Vigneresse, J. L., Barbey, P. & Cuney, M. (1996). Rheological Transitions During Partial Melting and Crystallization with Application to Felsic Magma Segregation and Transfer. *Journal of Petrology* **37**, 1579–1600.

Walker, B. A., Bergantz, G. W., Otamendi, J. E., Ducea, M. N. & Cristofolini, E. A. (2015). A MASH zone revealed: The mafic complex of the Sierra Valle Fértil. *Journal of Petrology* **56**, 1863–1896.

Wang, H., Currie, C. A. & DeCelles, P. G. (2015). Hinterland basin formation and gravitational instabilities in the central Andes: Constraints from gravity data and geodynamic models. In: DeCelles, P. G., Ducea, M. N., Carrapa, B. & Kapp, P. A. (ed.) *Geodynamics of a Cordilleran Orogenic System: The Central Andes of Argentina and North Chile*. The Geological Society of America **212**, 387-406.

Ward, K. M., Zandt, G., Beck, S. L., Christensen, D. H. & McFarlin, H. (2014). Seismic imaging of the magmatic underpinnings beneath the Altiplano-Puna volcanic complex from the joint

inversion of surface wave dispersion and receiver functions. *Earth and Planetary Science Letters* **404**, 43–53.

Watson, E. B. (1982). Melt infiltration and magma evolution. *Geology* **10**, 236–240.

Weber, M. B. I., Tarney, J., Kempton, P. D. & Kent, R. W. (2002). Crustal make-up of the Northern Andes: Evidence based on deep crustal xenolith suites, Mercaderes, SW Colombia. *Tectonophysics* **345**, 49–82.

Weinberg, R. F. & Hasalová, P. (2015). Water-fluxed melting of the continental crust: A review. *Lithos* **212**–**215**, 158–188.

White, A. J. R., Chappell, B. W. & Wyborn, D. (1999). Application of the restite model to the Deddick Granodiorite and its enclaves-A reinterpretation of the observations and data of Maas et al. (1997). *Journal of Petrology* **40**, 413–421.

White, R. W., Powell, R., Holland, T. J. B., Johnson, T. E. & Green, E. C. R. (2014). New mineral activity-composition relations for thermodynamic calculations in metapelitic systems. *Journal of Metamorphic Geology* **32**, 261–286.

White, R. W., Stevens, G. & Johnson, T. E. (2011). Is the crucible reproducible? Reconciling melting experiments with thermodynamic calculations. *Elements* **7**, 241–246.

Wolf, M. B. & Wyllie, P. J. (1991). Dehydration-melting of solid amphibolite at 10 kbar: Textural development, liquid interconnectivity and applications to the segregation of magmas. *Mineralogy and Petrology* **44**, 151–179.

Wolf, M. B. & Wyllie, P. J. (1993). Garnet growth during amphibolite anatexis: implications of a garnetiferous restite. *Journal of Geology* **101**, 357–373.

Wolf, M. B. & Wyllie, P. J. (1994). Dehydration-melting of amphibolite at 10 kbar: the effects of temperature and time. *Contributions to Mineralogy and Petrology* **115**, 369–383.

Wyllie, P. J. & Wolf, M. B. (1993). Amphibolite dehydration-melting: Sorting out the solidus. *Geological Society Special Publication* **76**, 405–416.

Yakymchuk, C. & Brown, M. (2014). Consequences of open-system melting in tectonics. *Journal of the Geological Society* **171**, 21-40.

Yang, J., Cao, W., Gordon, S. M. & Chu, X. (2020). Does Underthrusting Crust Feed Magmatic Flare-Ups in Continental Arcs? *Geochemistry, Geophysics, Geosystems* **21**, E2020GC009152.

Yoshino, T. & Okudaira, T. (2004). Crustal growth by magmatic accretion constrained by metamorphic P-T paths and thermal models of the Kohistan arc, NW Himalayas. *Journal of Petrology* **45**, 2287–2302.

Zandt, G., Gilbert, H., Owens, T. J., Ducea, M., Saleeby, J. & Jones, C. H. (2004). Active foundering of a continental arc root beneath the southern Sierra Nevada in California. *Nature* **431**, 41–46.

Zanetti, A., Mazzucchelli, M., Rivalenti, G. & Vannucci, R. (1999). The Finero phlogopite-peridotite massif: An example of subduction-related metasomatism. *Contributions to Mineralogy and Petrology* **134**, 107–122.

Zellmer, G. F. (2008). Some first-order observations on magma transfer from mantle wedge to upper crust at volcanic arcs. *Geological Society Special Publication* **304**, 15–31.

Zhang, J. & Green, H. W. (2007). Experimental investigation of eclogite rheology and its fabrics at high temperature and pressure. *Journal of Metamorphic Geology* **25**, 97–115.

Table 1: Bulk compositions (in wt.% oxide and normalized to 100%) used to model partial melting and crystallization in the deep crustal hot zone.
FeO_T is calculated as $FeO_T = FeO + 0.8998*Fe_2O_3$.

Lithology	Pressure (GPa)	Fluid content	SiO_2	TiO_2	Al_2O_3	FeO_T	MgO	CaO	Na_2O	K_2O	H_2O	O_2
Primitive arc basalt[a]	1.5	Fluid absent	50.39	0.97	14.43	9.07	11.30	9.72	2.63	-	1.50	-
	2.0		50.70	0.97	14.52	9.12	11.37	9.77	2.54	-	0.90	-
Metapelite[b]	1.5	Fluid absent	57.11	1.07	20.49	8.51	3.28	1.56	1.83	4.08	1.93	0.14
	2.0		57.23	1.07	20.53	8.52	3.29	1.57	1.83	4.09	1.73	0.14
Metagraywacke[c]	1.5	Fluid absent	64.59	0.56	15.52	5.61	3.49	2.69	3.90	1.98	1.56	0.09
	2.0		65.05	0.57	15.63	5.65	3.52	2.71	3.93	2.00	0.86	0.09

[a]Primitive calc-alkaline basalt from the Kamchatka arc (Schmidt & Jagoutz, 2017).
[b]Average composition of amphibolite-grade metapelite from Ague (1991) with $Fe^{3+}/(Fe^{2+}+Fe^{3+}) = 0.15$.
[c]Metagraywacke sample ES356 from Sawyer (1986) with $Fe^{3+}/(Fe^{2+}+Fe^{3+}) = 0.15$.

Figure Captions

Fig. 1. (a) Cartoon depicting the stages of the Cordilleran cycle. During (1) early recharge, retroarc shortening delivers melt-fertile lithosphere to the subarc region. Melting of this fertile lithosphere in the deep crustal hot zone (red box) leads to (2) high-flux magmatism, which generates a dense residual arclogitic root in the subarc lower crust. This root takes up space in the mantle wedge, restricts further retroarc underthrusting, and causes surficial subsidence and "bobber basin" formation. Because it is gravitationally unstable, the root founders into the asthenosphere. During the (3) waning stage of the high-flux event, lithospheric foundering and concomitant asthenospheric upwelling cause rapid surficial uplift, hinterland extension, and local basaltic volcanism. Creation of space in the mantle wedge allows renewed horizontal shortening, and the cycle begins again. Modified from DeCelles *et al*. (2015a). (b) Schematic of a deep crustal hot zone (Annen *et al*., 2006), the locus of intrusion of hot, hydrous mantle-derived basalt into the lower crust of an active arc. Here, fractional crystallization and partial melting act in concert to form the intermediate magmas of Cordilleran upper crustal batholiths. Based on Cashman *et al*. (2017).

Fig. 2. Density of the refractory subarc root *vs*. temperature for different percentages of trapped intermediate melt at (a) 1.5, (b) 2.0, and (c) 2.5 GPa. Shown in gray is the average density of the upper mantle (3.25-3.35 g/cm^3). The yellow region highlights the amount of melt seismically detected in the lower crust of the central Andean Cordillera (Delph *et al*., 2017). The average temperature of the lower crust (700-950^{o}C) is outlined in red.

Fig. 3. Volume % *vs*. temperature plots for an average water-undersaturated arc basalt at (a) 1.5 GPa and (b) 2.0 GPa. Densities of the total assemblage (solid red line) as well as the solid residual assemblage (dashed red line) are shown with corresponding values on the right y-axis. The gray region represents the average density of the upper mantle (3.25-3.35 g/cm^3). The region to the right of the vertical dashed line is the temperature range at which the solid residue has an average arclogitic mineralogy (equal proportions of garnet and clinopyroxene plus 0-10 vol.% amphibole; Ducea *et al*., 2021a). Mineral abbreviations for all figures are: Wm = white mica, Afs = alkali feldspar, Bt = biotite, Ky = kyanite, Sil = sillimanite, Amp = amphibole, Pl = plagioclase, Grt = garnet, Cpx = clinopyroxene, Qz = quartz, Rt = rutile.

Fig. 4. Cartoon depicting scenarios leading to the production of (a) density-unstable and (b) density-stable residues.

Fig. 5. Summary diagram showing the density ranges (in black) of basalt-derived cumulates as well as basaltic, metapelitic, and metagraywacke restites generated by our thermodynamic models. Densities of basaltic restites are broken up into those that are density-unstable (melt-depleted restites at all pressures + melt-fertile restites at 2 GPa; solid line) and those that extend to densities lower than that of the mantle (only melt-fertile restites at 1.5 GPa; dashed line). For comparison, shown in red is the average density range of natural arclogites from Ducea (2002)[1] and Jagoutz & Schmidt (2013)[2]. Light blue points are tonalite restites formed experimentally by Patiño Douce (2005)[3] at 1.5 and 2.1 GPa from 940-1060^{o}C. The one light blue point with a density greater than the upper mantle was partially melted at 1060^{o}C, the highest investigated temperature. Dark blue points are natural tonalite restites from Hacker *et al*. (2005)[4]. Shown in green are the densities of sanidine eclogites from the Pamir interpreted by Hacker *et al*. (2005) as

metapelitic restites. Purple points are restites of biotite-bearing, Ti-rich, Al-poor metagraywacke experimentally melted at 1.5 and 2 GPa with densities calculated using Abers & Hacker (2016). Dark purple points are densities of biotite gneiss-derived restites from Patiño Douce & Beard (1995). Density-unstable restites form where high temperatures (>975^{o}C) cause full consumption of biotite. Light purple points are from Auzanneau *et al*. (2006).

Fig. 6. Volume % *vs*. temperature plots for an average water-undersaturated arc basalt undergoing partial melting at 1.5 GPa and 2.0 GPa. (a, c) Open-system partial melting and cyclic melt extraction at 7 vol.% (melt connectivity transition). Dashed vertical lines represent melt loss events. (b, d) Phase equilibria of the melt-depleted residue. Densities of the total assemblage (solid red line) as well as the residual mineralogy (dashed red line) are shown with corresponding values on the right y-axis. The gray region represents the average density of the upper mantle (3.25-3.35 g/cm^3). See Figure 3 for mineral abbreviations.

Fig. 7. As in Figure 6, but for an average water-undersaturated metapelite. See Figure 3 for mineral abbreviations.

Fig. 8. As in Figure 6, but for an average water-undersaturated metagraywacke. See Figure 3 for mineral abbreviations.

Fig. 9. (a) Cartoon showing the density and thickness structure of a Cordilleran arc (right) relative to average continental crust (left). Shown in gray is the subarc lower crustal root, which may be composed of arclogite. We vary the thickness and density of the lower crust from 1-20 km and 2.9-3.5 g/cm^3, respectively, while maintaining the crustal thickness of the bulk arc at 50

km. The upper crust of the arc is varied from 30-49 km and has a density of 2.775 g/cm^3 (Hacker *et al*., 2015). The density and thickness of the average continental crust are taken, respectively, as 2.87 g/cm^3 (Lee *et al*., 2015) and 36.1 km (Hacker *et al*., 2015). The density of the upper mantle down to the compensation depth is assumed to be 3.3 g/cm^3. (b) Plot depicting how the elevation of the arc (H) relative to average continental crust varies as a function of the thickness (1-20 km) and density (2.9-3.5 g/cm^3) of the lower crustal root. See text for detailed explanation.

Fig. 10. Elevation *vs*. crustal thickness for all continental regions. Crustal thickness data is from the Crust 1.0 model (https://igppweb.ucsd.edu/~gabi/rem.html; Laske *et al*., 2013) and elevation data is from the 1 arc-minute ETOPO1 global relief model for bedrock (https://www.ngdc.noaa.gov/mgg/global/). Vertical dashed lines are drawn to bracket the elevation range of 50-55 km-thick crust.

Fig. 1.

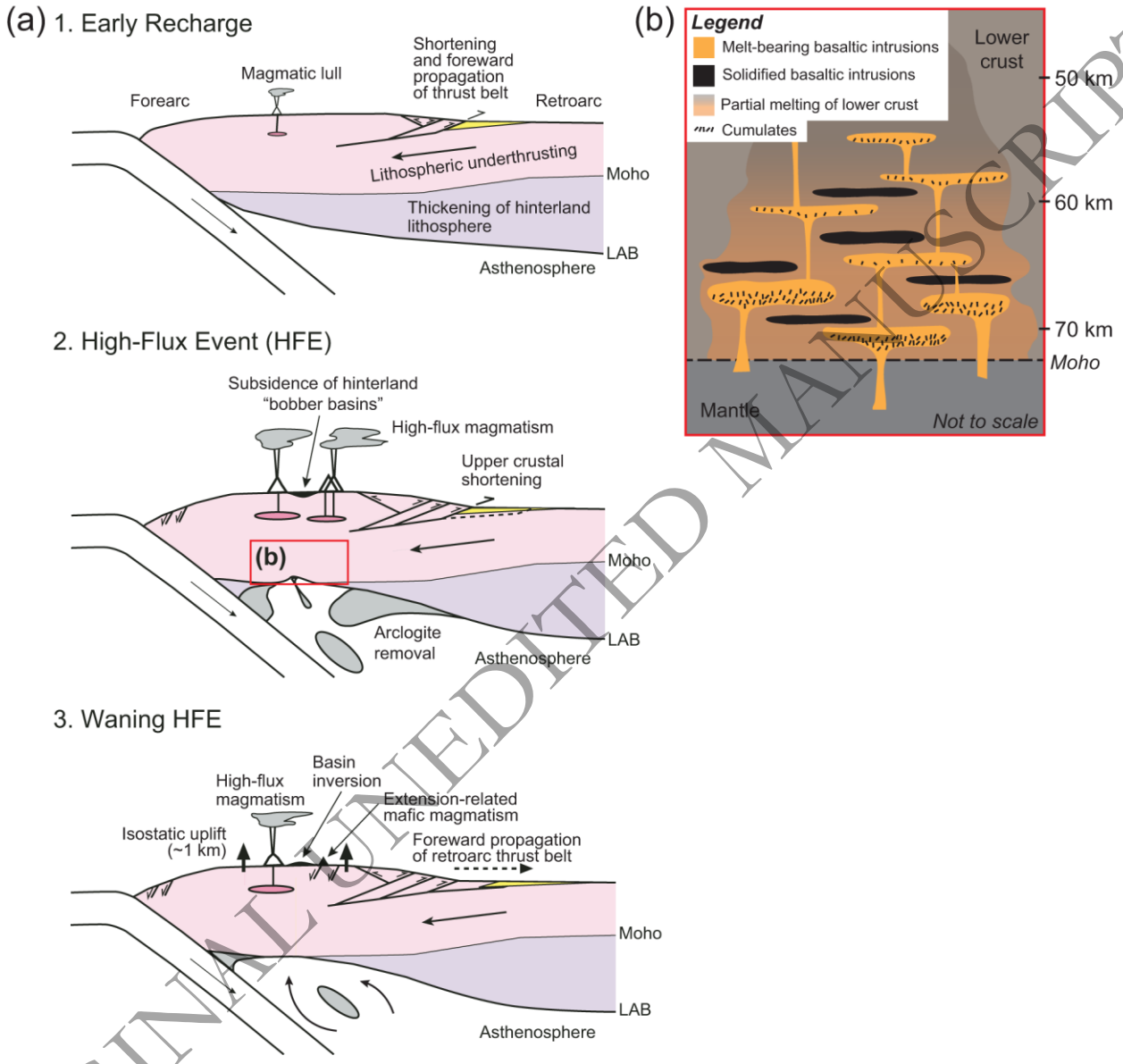

Fig. 2.

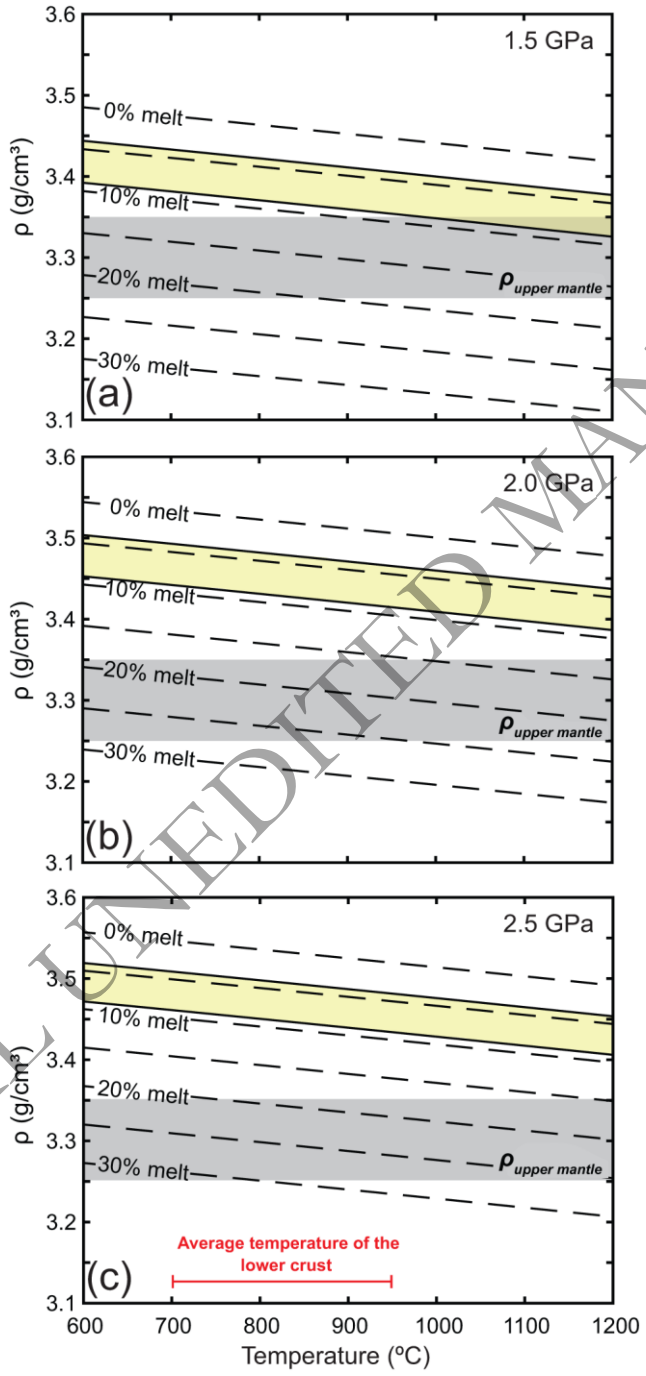

Fig. 3.

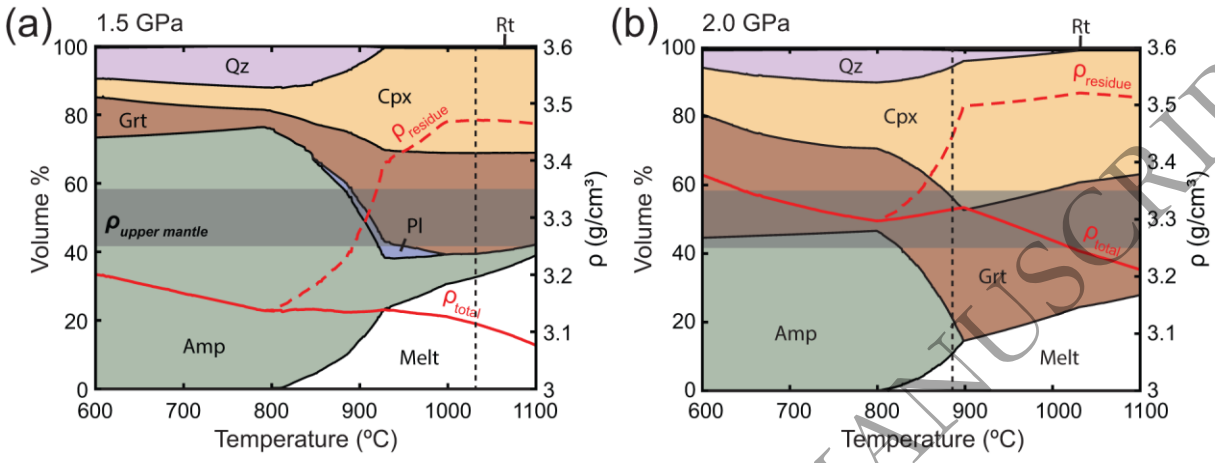

Fig. 4.

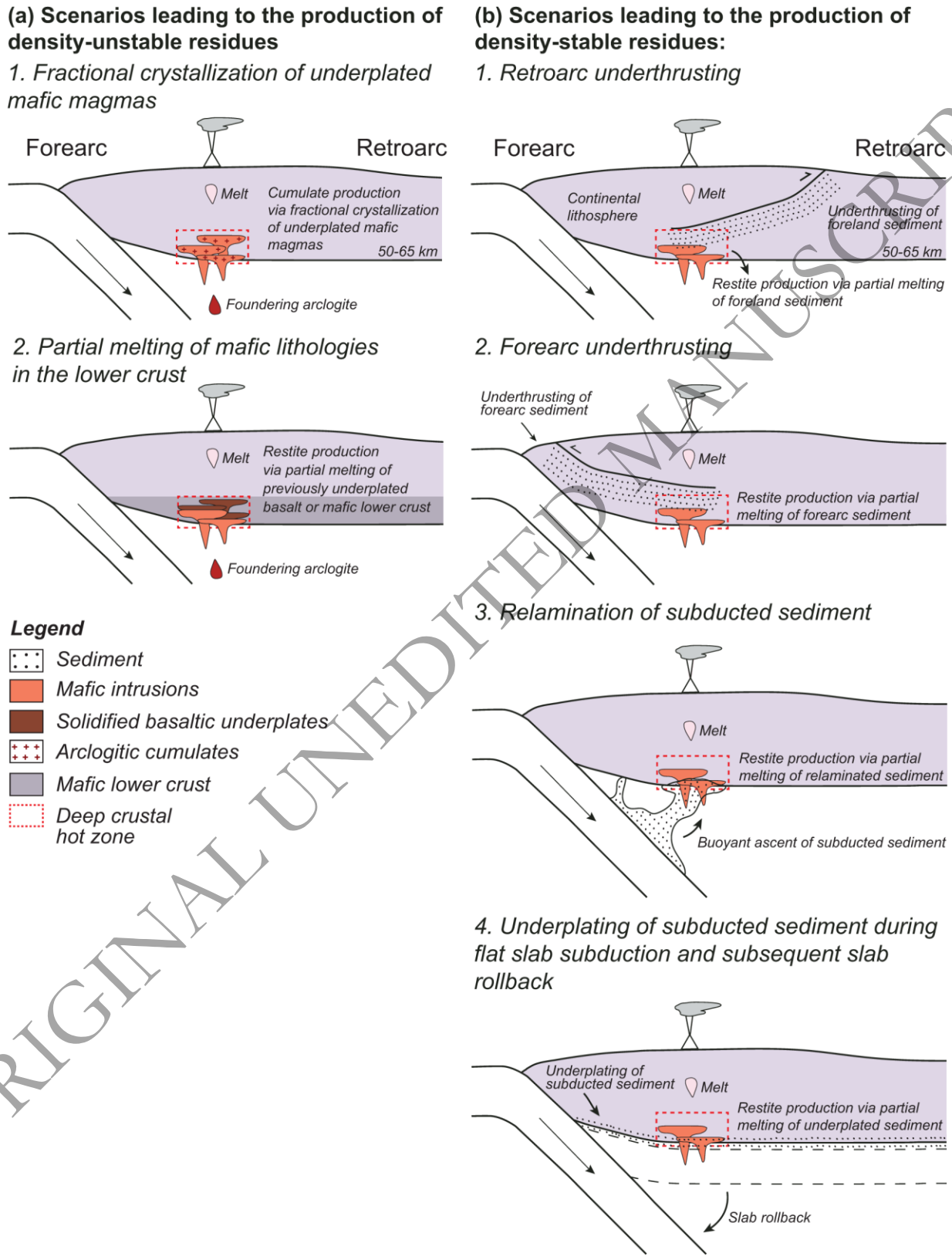

Fig. 5.

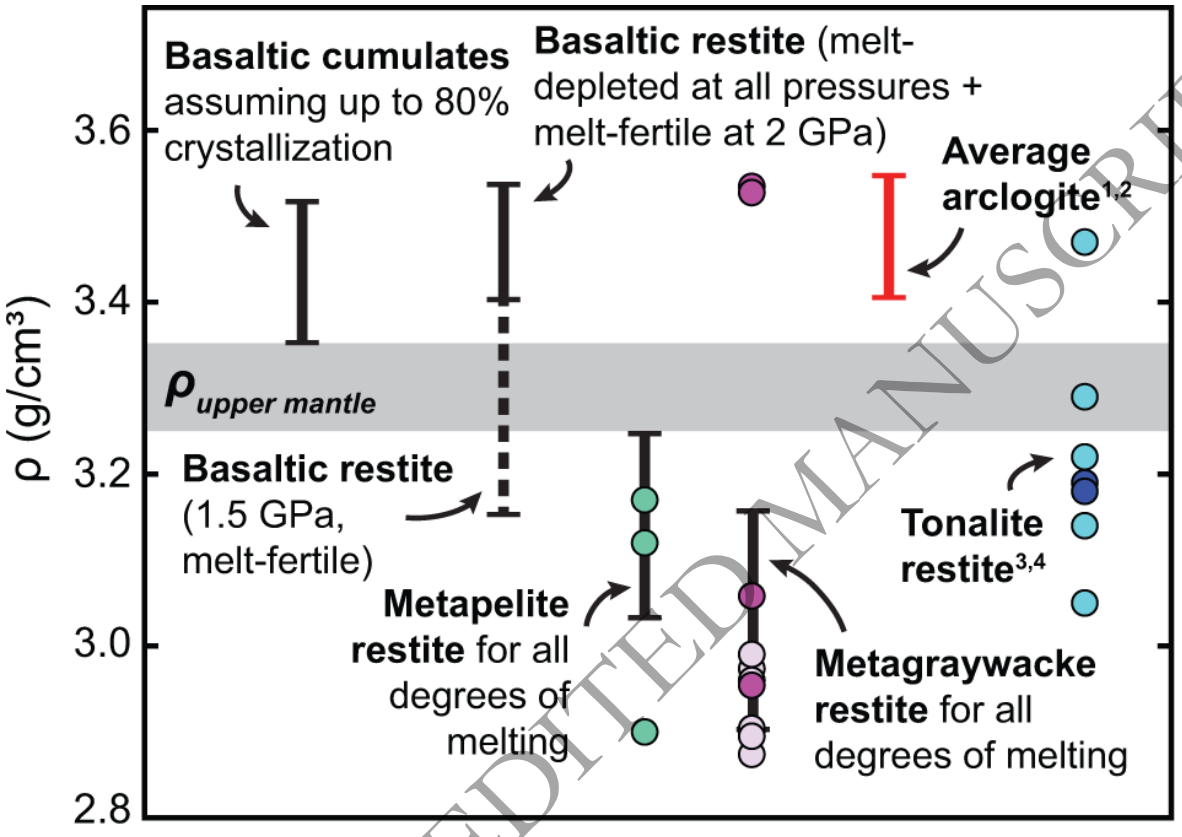

Fig. 6.

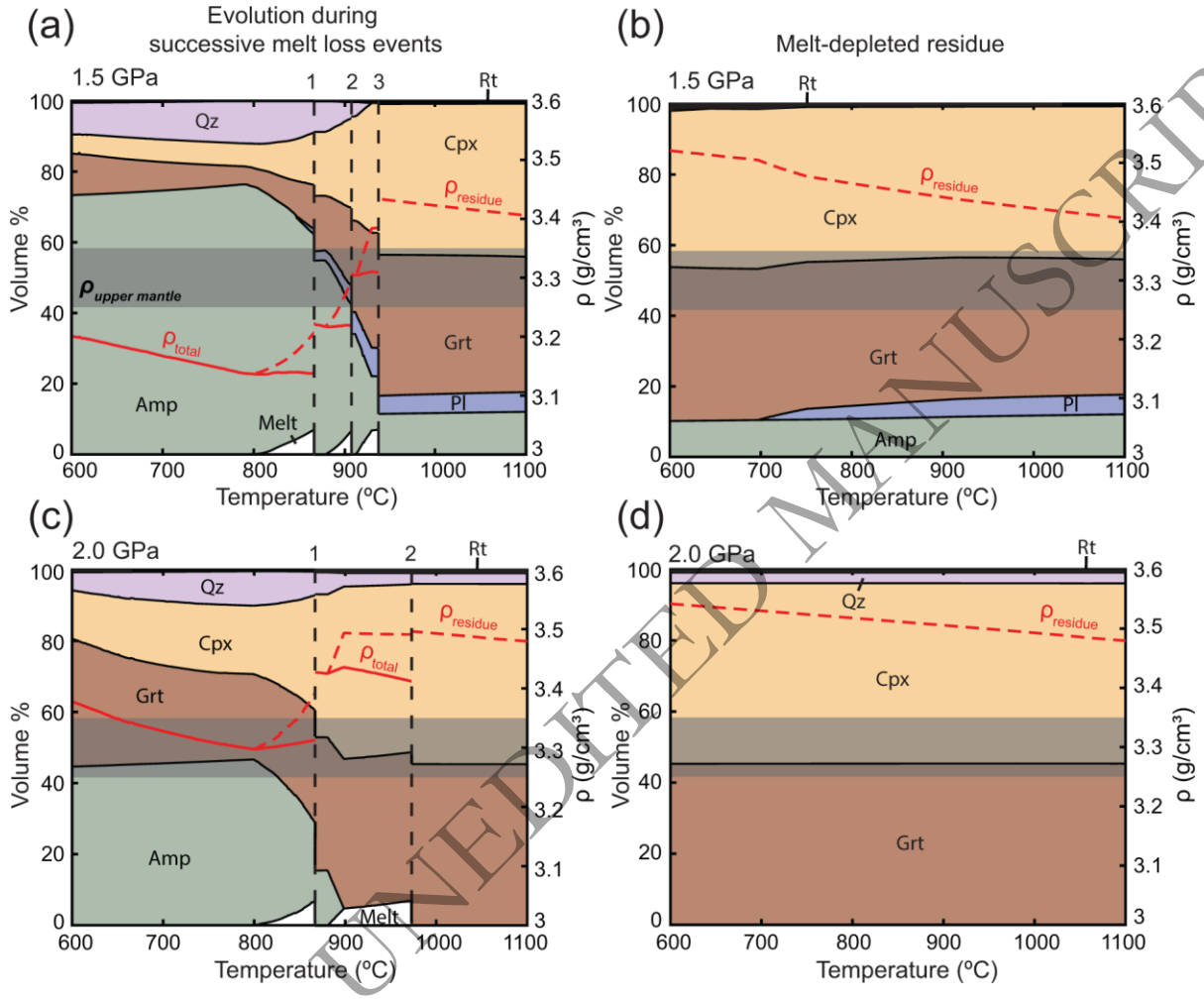

Fig. 7.

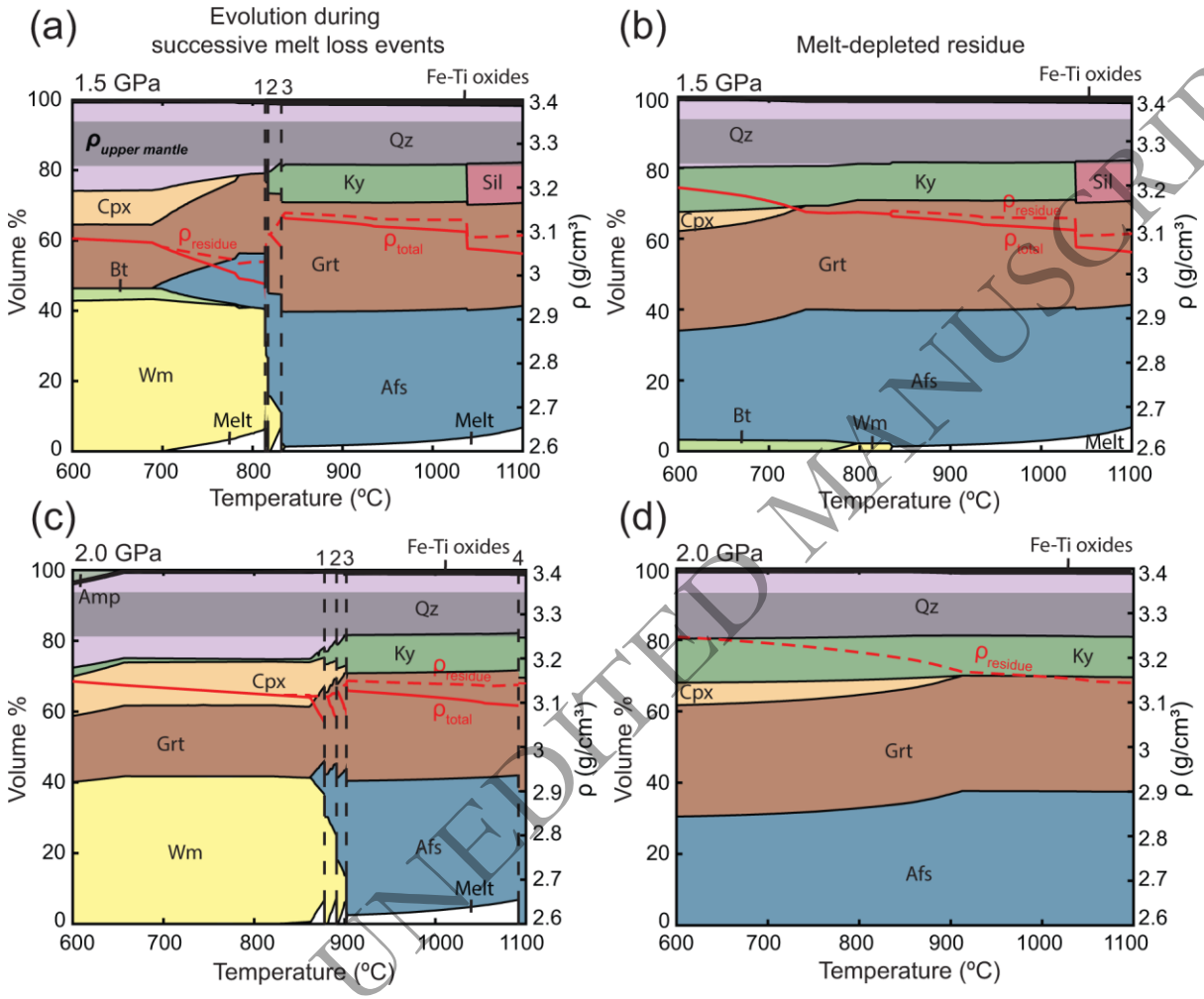

Fig. 8.

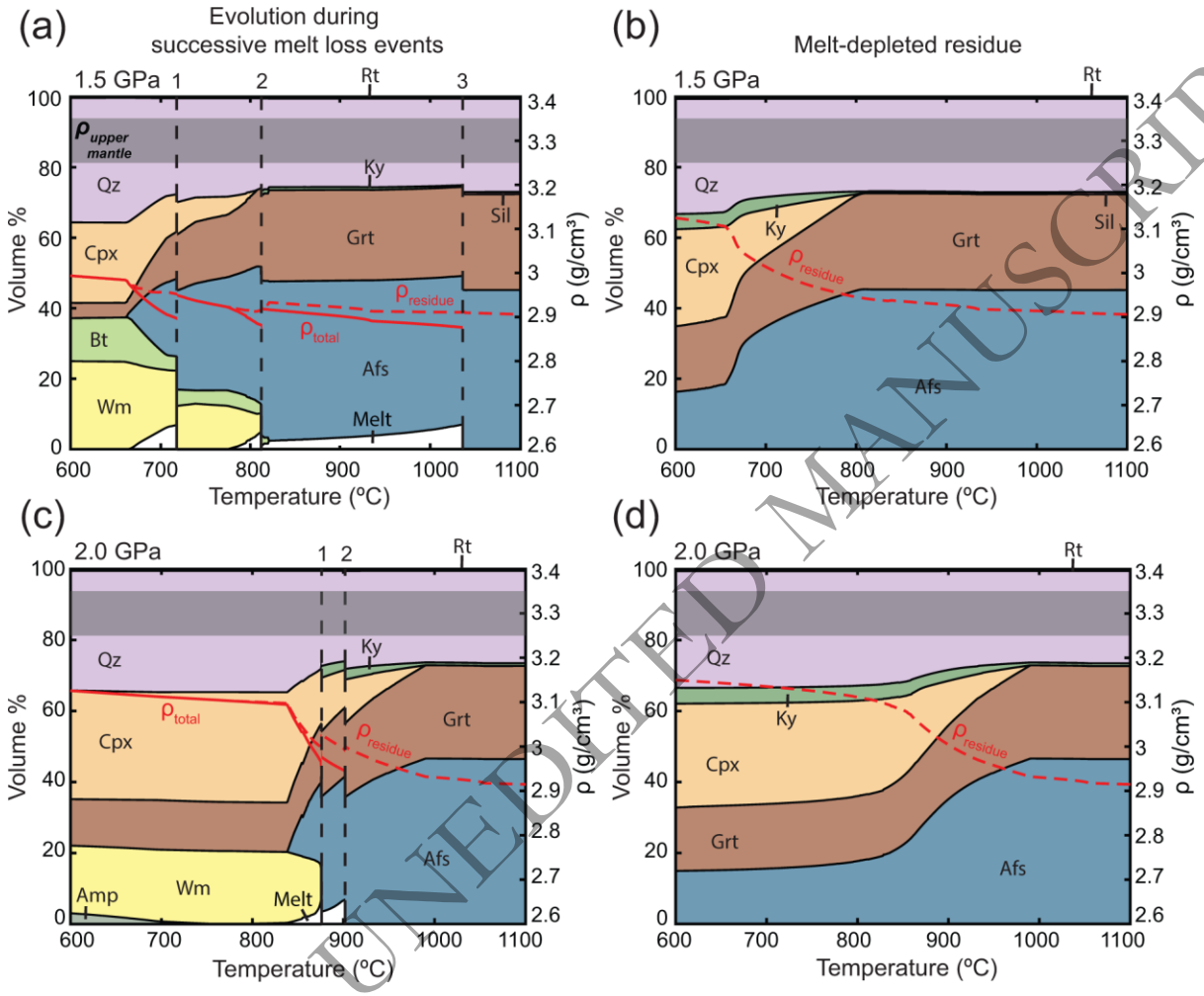

Fig. 9.

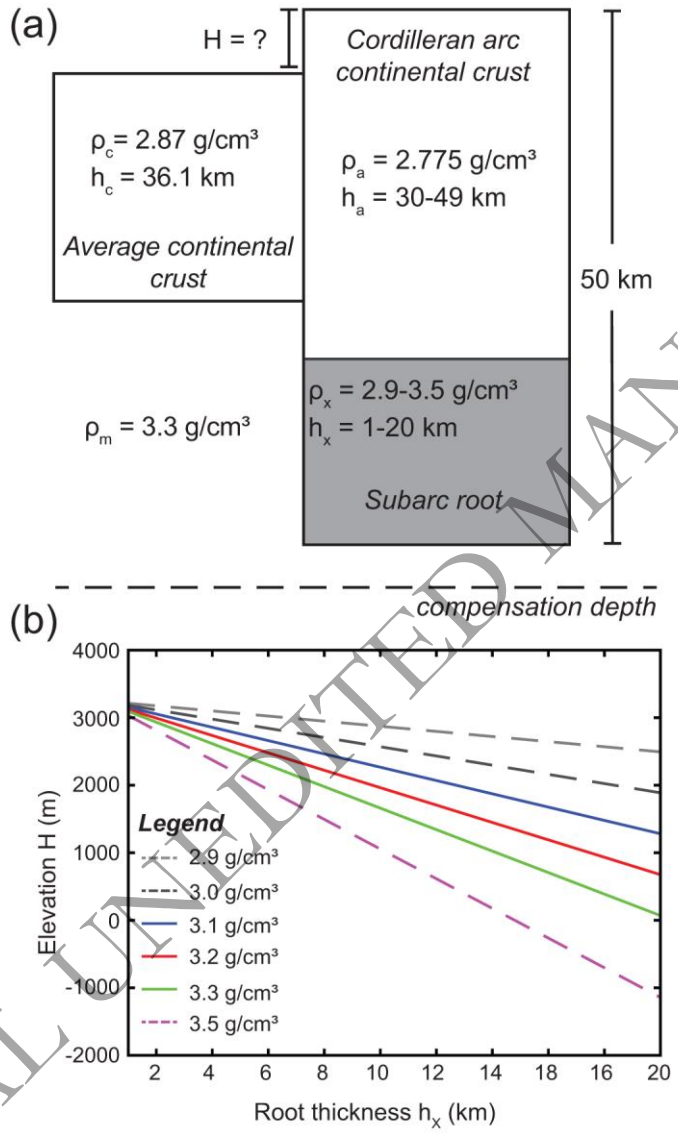

Fig. 10.